RICE UNIVERSITY

PRANDTL-MEYER EXPANSION OF IONIZED ARGON WITH DIFFERING ELECTRON AND ATOM TEMPERATURES

by

KENNETH L. KRAMER

A THESIS SUBMITTED
IN PARTIAL FULFILLMENT OF THE
REQUIREMENTS FOR THE DEGREE OF

MASTER OF SCIENCE

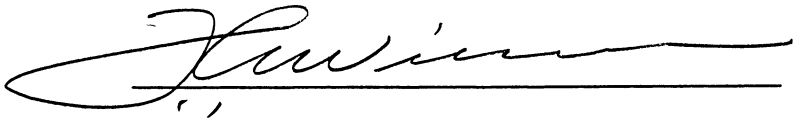

Houston, Texas

May, 1965

Kenneth La Cour Kramer

ABSTRACT

The sharp corner expansion of ionized argon with differing electron and atom temperatures has been calculated. The thermodynamic equations which apply for a two-temperature gas were derived. An energy balance on the electrons was performed to obtain a functional relationship between T_a, T_e, ρ, and α. The governing quasi-linear partial differential equations were solved by the Method of Characteristics.

The results obtained demonstrate that while $T_e \cong T_a$ throughout the expansion fan, the pressure, temperature, and degree of ionization are underestimated if the two temperatures are assumed equal during the solution of the problem.

ACKNOWLEDGEMENTS

The author would like to express his most sincere appreciation to Dr. Fredrick A. Wierum, Jr. of Rice University for the many hours of consultation and for the most invaluable suggestions given by him during the writing of this thesis. Special appreciation is expressed to The National Science Foundation which sponsored this research under Grant No. GP 2361, "Prandtl-Meyer Flow of Chemically Reacting Gases."

TABLE OF CONTENTS

LIST OF SYMBOLS

a	frozen speed of sound = $\sqrt{5/3(T_a + \alpha T_e)}$
E	internal energy of system
e	charge on an electron
$\bar{e}$	specific internal energy
G	Gibb's free energy
g_i^j	degeneracy of a particle of species i in energy level j
h	Planck's constant = 6.624×10^{-27} erg-sec.
$\bar{h}$	specific enthalpy
K	equilibrium constant
k	Boltzmann's constant = 1.3803×10^{-16} erg/^oK.
k_i	ionization rate constant
k_r	recombination rate constant
M	frozen Mach number
m	mass of a particle
N	number density of species denoted by subscript
N_o	Avagadro's number = 6.023×10^{23} 1/mole
n	normal coordinate
p	pressure
R	gas constant = 2.0813×10^6 erg/gm.-^oK.
S	entropy of system
s	specific entropy
T	temperature

LIST OF SYMBOLS (con't.)

Tx	134,000 °K.
u	velocity
V	volume
$\dot{w}$	mass production rate
x,y	dimensional orthogonal coordinates
Z	partition function
α	degree of ionization = $N_e/(N_a + N_e)$
β	$= A_e A_{a+} / A_a$
γ	isentropic index = 5/3
δ	defined by equations (7.2a) and (7.2b)
ϵ	energy reference level
ξ, η	nondimensional coordinates
ϕ	$= T_a + \alpha T_e$
ρ	density
μ	angle between characteristic and velocity vector, chemical potential
θ	angle between horizonal and velocity vector
χ	ionizational potential

SUBSCRIPTS

a	atom
a+	ion
c	characteristic quantity defined in Section IV

SUBSCRIPTS (con't.)

e	electron
i	a general species
o	stagnation quantity
s	the streamline intersection
*	equilibrium quantity
1	free stream condition
I	the number of the point out on a characteristic
J	the number of the characteristic

SUPERSCRIPTS

elec	electronic energy or energy mode
o	ground state
rot	rotational energy mode
tr	translational energy mode
vib	vibrational energy mode
"	excited state

I INTRODUCTION

The high stagnation enthalpies of the gases flowing about hypervelocity vehicles give rise to such chemical reactions as dissociation, ionization, and/or recombination. Because extremely high temperatures and low static pressures usually accompany such flows, investigation of the departures from equilibrium in these flows become important in their analysis. The reaction rates are intimately related to the rates of collision between the elementary gas particles; hence, they are strongly coupled to the gas density which is usually low.

This thesis treats the supersonic expansion of an ionizing monatomic gas around a sharp corner. Shock waves have been treated in references 20 and 23, and nozzle flows in references 5 and 6. The equations governing the flow field are partial differential equations which may be solved by the Method of Characteristics. Argon was chosen as the working fluid because of its widespread use in shock tubes, plasma jets, hypersonic wind tunnels, and magnetohydrodynamic generators, in each of which ionization and recombination are important.

Classical Mechanics shows that the fraction of energy transferred between two particles in an elastic collision is approximately equal

to their mass ratio. Because gaseous atoms and ions have essentially the same mass, only a single collision between these particles is required to equilibrate their kinetic energy or equalize their temperatures ($T_a = T_{a+}$). However, in elastic collisions between atoms (or ions) and electrons only small amounts of energy are transferred since the mass of the electron is infinitesimal compared to that of the atom. Generally, then, the temperature of the electron gas is different from that of the atom and ion gas. However, in section III it will be shown that the temperatures of all the elementary particles must be equal when the flow is in equilibrium.

Several different mechanisms of ionization and recombination of monatomic gases have been postulated. In this thesis, the reaction rates will be determined by use of a Thompson three-body collision mechanism, an electron serving as the third body. Radiative and dissociative recombination are neglected since they have been shown to be of secondary importance at moderate electron densities (2,23)*. The reaction rates used in this analysis are essentially those of Petschek and Byron (23) corrected for the effects of recombination.

Other simplifying assumptions include neglecting the effects of conductive, convective, and radiative heat transfer. Processes involving diffusion and viscosity are neglected, so the fluid remains

---

*Numbers in parenthesis refer to references on page 59.

electrically neutral ($N_{a+} = N_e$). Only steady flow will be considered.

Originally this work was to include consideration of the excited states of the argon atom and ion (Appendix I), but initial investigations of their influence indicated the increased complexity to be unnecessary. Figure 5 illustrates the slight differences in the internal energy and in the equilibrium composition which result from neglecting the excited states. Thus, all particles will be assumed to be in their ground state.

The temperature range of this investigation is:

$$8000^{\circ}K. < T_a < 15,000^{\circ}K.$$

Below 8000°K. the three-body collision process is not the predominant mechanism of recombination (23), and above 15,000°K. multiple ionization becomes important (12).

Coulomb forces due to the charges on the ions and electrons are included in performing the electron energy balance and in evaluating the expression for the recombination rate coefficient; otherwise they are neglected. Dougal and Goldstein (11) have shown that the characteristic time for the equipartition of excess electron energy is 5 microseconds if Coulomb forces are considered and 160 microseconds if they are neglected. Experimental data more closely approximate the former value, thus the inclusion of Coulomb forces in these instances is mandatory.

Prandtl-Meyer flow is the steady, supersonic expansion of a gas about a sharp two-dimensional corner. If the flowing gas does not chemically react, or if the reactions are either frozen or in equilibrium, no characteristic length enters the problem and all fluid dynamic properties may be assumed independent of the radial distance from the corner. Reacting gas flows, however, have a characteristic chemical time (τ_c), which implies a characteristic length so the properties are functions of the radial position distance from the corner. At the corner, τ_c is very large compared to the flow time, hence the composition of the gas may be assumed to be unchanging, i.e., "frozen." At some distance ftom the corner, the flow time will become negligible compared to the characteristic chemical time, and the gas will undergo an equilibrium expansion. At intermediate positions in the expansion fan, then, the flow may be expected to depart from equilibrium. It is this region of non-equilibrium flow which is investigated in this thesis.

In the following section, the thermodynamic equations required for the solution of this problem are presented. These include the mass species production equation which is required since chemical reactions are considered. Also presented is the electron energy balance from which the relation between T_a and T_e, ρ, and α is obtained. Formulation of the solution of the governing equations

by the Method of Characteristics is outlined in Section V, and the frozen Prandtl-Meyer flow solution is presented in Section VI. This solution provides boundary conditions at the corner for the nonequilibrium flow solution. The technique used in the numerical integration of the governing differential equations is presented in Section VII. Results obtained for the particular cases calculated are discussed in Section VIII and conclusions are presented in Section IX.

II THERMODYNAMIC EQUATIONS

(1) THE EQUATION OF STATE

Kinetic theory gives as the basic relationship between the pressure, temperature and volume of a mixture of perfect gases (20):

$$p_i V = 1/3\, N_i m_i u_i^2 = N_i k T_i \tag{2.1}$$

Summing this equation over all species and employing Dalton's law for partial pressure gives:

$$pV = k(N_a T_a + N_e T_e + N_{a+} T_{a+}) \tag{2.2}$$

If the mass of the electron is neglected, the total mass of the system may be represented by:

$$\rho V = N_a m_a + N_{a+} m_{a+} = m_a(N_a + N_{a+}) \tag{2.3}$$

From the assumptions of electrical neutrality and equal atom and ion temperatures, the equation of state becomes:

$$p = \rho \frac{k}{m_a}(T_a + \alpha T_e) \tag{2.4}$$

where the usual definition of the degree of ionization has been employed:

$$\alpha = \frac{N_e}{N_a + N_e}$$

(2) THE ENERGY EQUATION

A complete derivation of the energy equation is given in Appendix I, the discussion here is for the unexcited monatomic gas.

Statistical thermodynamics gives the relationship between the partition function and the internal energy of a particle as:

$$E = k T \left[\frac{\partial \ln(Z_i)}{\partial T_i}\right]_v = \frac{kT_i}{Z_i}\left[\frac{\partial Z_i}{\partial T_i}\right]_v \tag{2.5}$$

The straight forward differentiation of the partition function, equation (1.6), yields from (2.5) the internal energy per particle of species i as:

$$E_i = 3/2\ k\ T_i + \epsilon_i^o \tag{2.6}$$

Summing over all species noting that $T_a = T_{a+}$ and $N_{a+} = N_e$, the energy of the mixture becomes:

$$E = 3/2\ k\ \left[(N_a + N_e)T_a + N_e T_e\right] + N_a \epsilon_a^o + N_e(\epsilon_e^o + \epsilon_{a+}^o) \tag{2.7}$$

If the ground state of the atom, ϵ_a^o, is defined as the zero energy reference, then $(\epsilon_{a+}^o + \epsilon_e^o) = \chi$, the ionization potential. Thus, the specific internal energy may be written as:

$$\bar{e} = 3/2\ \frac{k}{m_a}(T_a + \alpha\ T_e) + \frac{\alpha\ \chi}{m_a} \tag{2.8}$$

Use of the thermodynamic definition of enthalpy with equation (2.4) gives for the specific enthalpy:

$$\bar{h} = 5/2 \frac{k}{m_a}(T_a + \alpha T_e) + \frac{\alpha \chi}{m_a} \tag{2.9}$$

Since the gas originates from a region of steady, uniform, equilibrium flow and expands adiabatically, the total enthalpy must be conserved. That is:

$$H_o = \bar{h} + 1/2\, u^2 = \text{Constant} \tag{2.10}$$

(2) SPEED OF SOUND

The speed of propagation of an infinitesimally small disturbance in a reacting gas has been the subject of much analytic investigation. For the two-temperature gas used in this thesis, Bray and Wilson (6) have shown that the frozen speed of sound may be obtained by elimination between the continuity and momentum equations. Their result is:

$$a^2 = 5/3\, (T_a + \alpha T_e) \tag{2.11}$$

III GAS DYNAMIC EQUATIONS

The equations expressing the conservation of mass and momentum of a reacting gas flow are the same as those derived assuming a perfect gas. Expressed in normal (n) and streamline (s) coordinates, the governing gas dynamic equations are (17, 18):

(1) THE OVERALL CONTINUITY EQUATION

$$\frac{\partial (\rho u)}{\partial s} + \rho u \frac{\partial \theta}{\partial n} = 0 \tag{3.1}$$

(2) THE S-MOMENTUM EQUATION

$$u \frac{\partial u}{\partial s} + \frac{1}{\rho} \frac{\partial p}{\partial s} = 0 \tag{3.2}$$

(3) THE N-MOMENTUM EQUATION

$$u^2 \frac{\partial u}{\partial s} + \frac{1}{\rho} \frac{\partial p}{\partial n} = 0 \tag{3.3}$$

These equations, however, are not sufficient to specify completely the state of the gas. The chemical reactions require that a species mass conservation equation be obtained.

(4) THOMPSON THREE BODY COLLISIONS

In the reaction equation:

$$A_r^+ + e + M \underset{k_r}{\overset{k_i}{\rightleftharpoons}} (A_r^o)'' + M + (K.E.)_m \tag{3.4}$$

a high energy electron collides with a third body (an atom, ion, or

another electron) in the presence of an ion. Due to the Coulombic attraction, the ion and electron combine to form a neutral atom, which may exist in an excited state (denoted by the double prime). The energy lost by the electron appears as the kinetic energy of the third body, M. The electron is not permanently captured until it reaches a bound state in the atom which lies at least kT_e below the ionization limit. The presence of the third body is necessary to reduce the energy of the electron sufficiently so that this recombination may occur.

Petschek and Byron (23) have shown that 90% of the ionization behind strong shock waves in argon is a result of three-body collisions. Since this form of the reaction has been shown to be predominant at high electron densities (2, 23), the stabilizing third body is assumed to be an electron. With this assumption, (3.4) becomes:

$$A_r^+ + e^- + e^- \underset{k_i}{\overset{k_r}{\rightleftharpoons}} (A_r^o)'' + e^- + (K.E.)_{e^-} \tag{3.5}$$

The excess translational energy of the colliding electron is transferred to the "third-body" electron, and the energetic insulation between atoms and electrons allows their temperatures to differ by a significant amount. Due to its small mass, the mobility of the electron is much greater than that of the atom or ion. Consequently, the collision mechanism and the rates of reaction are strongly dependent on the electron temperature, as will be shown in section III-7.

(5) THE SAHA EQUATION

The thermodynamic requirement for equilibrium at a fixed pressure and the temperature is that the Gibb's free energy be a minimum for all possible changes of mass. This statement can be written as:

$$\Delta G = \sum \upsilon_i \mu_i = 0 \tag{3.6}$$

where ν_i is the stoichiometric coefficient of the i^{th} species in the reaction and μ_i is its chemical potential. For the reaction represented by (3.5), this becomes:

$$\mu_a = \mu_e + \mu_{a+} \tag{3.7}$$

The chemical potential, μ_i, may be calculated from the partition function:

$$\mu_i = -RT_i \ln (Z_i) \tag{3.8}$$

Substitution of (1.2, (1.3) and (1.8, (1.9, and (1.10) into (3.8) gives a functional relationship between the equilibrium composition of the mixture and its temperature and density. This expression, called the Saha equation, for an ionizing monatomic gas with excited states is:

$$\frac{\alpha_*^2}{1 - \alpha_*} = (g_e{}^o)\, B \left[\frac{Z_{a+}^{elec}}{Z_a^{elec}}\right] \frac{T_*^{3/2}}{\rho} \exp (-\chi / kT_*) \tag{3.9}$$

Where g_e^o is the degeneracy of the electron's ground state and

$B = (\frac{2 \pi k m_e}{h^2})$ $m_a \cdot Z_a$ and Z_{a+} are the electronic partition functions of the atom and ion respectively. Figure 5 shows that the excited states have little effect on the equilibrium composition in the temperature range 8,000-15,000°k, so:

$$\frac{\alpha_*^2}{1 - \alpha_*} = \frac{T_*^{3/2}}{\rho} \exp(-\chi / kT_*) \quad \beta \tag{3.10}$$

where:

$$\beta = \frac{A_e A_{a+}}{A_a}$$

$$A_i = g_i^o \left(\frac{2 \pi m_i k}{h^2}\right)^{3/2} \tag{3.11}$$

Further information on these two material constants is given by Wierum in reference 27.

(6) MASS SPECIES PRODUCTION EQUATION

If the Law of Mass Action is applied to the reactions:

$$A_r^o + e^- \underset{k_r}{\overset{k_i}{\rightleftharpoons}} A_r^+ + e^- + e^- \tag{3.5}$$

the expression for the rate of production of electrons becomes:

$$\frac{D[e^-]}{Dt} = k_i [A_r^o][e^-] - k_i [A_r^+][e^-][e^-] \tag{3.12}$$

The brackets [ ] denote molar concentrations; k_i and k_r are constants of proportionality which depend on the collision mechanism

assumed for the elemental particles. D/Dt is the substantial derivative, here used in normal - streamline coordinates.

The molar concentrations of the various particles are

$$(3.13) \qquad \left[A_r^+\right] = \left[e^-\right] = \frac{\rho\,\alpha}{N_o m_a} \qquad \left[A_r^o\right] = \frac{\rho\,(1-\alpha)}{N_o m_a}$$

where electrical neutrality has been assumed. The equilibrium constant may be defined by:

$$(3.14) \qquad K_* = \frac{k_i}{kr} = \frac{\left[e^-\right]^2}{\left[A_r^o\right]} = \frac{\rho}{N_o m_a} \quad \frac{\alpha_*^2}{1-\alpha_*}$$

which, by use of the Saha Equation, may be written as:

$$(3.15) \qquad K_* = \frac{\beta}{N_o m_a} T_e^{3/2} \exp\left(-\chi / kT_e\right)$$

Substitution of (3.13a, (3.13b), and (3.14) into (3.12) gives:

$$(3.16) \qquad \frac{D(\rho\,\alpha)}{Dt} = k_r \frac{\rho^3\,\alpha}{(N_o m_a)^2}\left[\frac{\alpha_*^2}{1-\alpha_*}(1-\alpha) - \alpha^2\right]$$

Expanding the derivative and using the overall continuity equation, (3.1), the rate of production equation becomes (17):

$$(3.17) \qquad u\frac{\partial\alpha}{\partial s} = k_r \frac{\rho^2\alpha}{(N_o m_a)^2}\left[\frac{\alpha_*^2}{1-\alpha_*}(1-\alpha) - \alpha^2\right]$$

An expression for k_r must yet be derived.

(7) RECOMBINATION RATE CONSTANT: (k_r)

Assuming that atoms are initially rased to their first excited state and that every excited atom is subsequently ionized by an inelastic three-body collision with an electron, the rate of excitation

becomes the governing mechanism for ionization. By use of an empirical estimate of the inelastic cross section for collision, Petschek and Byron (23) give as the rate of ionization behind a strong shock in argon:

$$(3.18)\quad \frac{DNe}{Dt} = 4.4 \times 10^{-6} \frac{2\,k^3}{m_e \pi}\, T_e^{3/2} \left[\frac{T_x}{T_e} + 2\right] N_a\, N_e \exp(-T_x/T_e) \text{cm}^3/\text{sec}$$

The number densities of the atoms and electrons are N_a and N_e respectively. T_x is the energy of the first excited state expressed as a temperature. The first excited state of the argon atom is 11.5 e.v., or $T_x = 134{,}000^\circ K$.

Comparing (3.18) with (3.12), the ionization rate constant becomes (24):

$$(3.19)\quad k_i = 1.87 \times 10^{-16}\, T_e^{3/2} \left[\frac{T_x}{T_e} + 2\right] \exp(-T_x/T_e) \quad \text{cm}^3/\text{sec}$$

Rearrangement of (3.14) and substitution of the Saha Equation gives the recombination rate coefficient for argon as:

$$(3.20)\quad k_r = \frac{k_i}{K_*} = 6.5 \times 10^{-33} \left[\frac{T_x}{T_e} + 2\right] \exp\left(\frac{T_{ion} - T_x}{T_e}\right) \quad \text{cm}^3/\text{sec}$$

To aid in defining non-dimensionalizing parameters, it is advantageous to write k_r as the product of a dimensional term, k_{rd}, and a non-dimensional term, k_r'. Thus:

$$(3.21)\qquad k_r = k_{rd} \times k_r'$$

By use of Avogadro's number, N_o, k_{rd} may be expressed in terms of moles:

(3.22) $$k_{rd} = 2.358 \times 10^{15} \text{ cm}^6/\text{mole}^2\text{-sec}$$

while k_r' remains:

(3.23) $$k_r' = \left[\frac{T_x}{T_e} + 2\right] \exp\left(\frac{T_{ion} - T_x}{T_e}\right)$$

As suggested in Section III-4, the recombination rate constant is strongly dependent upon the electron temperature.

(8) ELECTRON ENERGY BALANCE

An electron energy balance may be expressed as:

(3.24) (rate of energy stored) = (rate at which energy is gained) - (rate at which energy is lost)

Neglecting heat transfer and other dissipative mechanisms, electrons are found to lose energy (E_{in}) in inelastic, ionizing, collisions with atoms and gain energy (E_{el}) in elastic collisions with atoms and ions. Equation (3.24) becomes:

(3.25) $$3/2\ N_e k \frac{dT_e}{dt} = E_{el} - E_{in}$$

The rate at which electrons lose energy due to ionizing collisions with atoms is:

(3.26) $$E_{in} = (\chi + 5/2\ kT_e)\frac{d\alpha}{dt} = k\,(T_{ion} + 5/2\ T_e)\frac{d\alpha}{dt} \quad \text{erg/cm}^3\text{-sec}$$

Since elastic collisions of electrons are 10^3 times more likely with ions than with atoms (23), the influence of atom-electron collisions upon this energy term are neglected. Reference 24 gives the energy transfer for elastic electron-ion collisions under the influence of Coulomb interaction as:

$$(3.27) \quad E_{el} = 2 \frac{N_e^2 e^4}{m_a} \left(\frac{8\pi m_e}{kT_e}\right)^{1/2} \left[\frac{T_a}{T_e} - 1\right] \ln\left[\frac{9(kT_e)^3}{8\pi N_e e^6}\right] \text{erg/cm}^3\text{-sec}$$

Compared to the right side, the magnitude of the left side of (3.25) is negligible. With this assumption, the electron energy balance becomes:

$$(3.28) \quad E_{el} = E_{in}$$

which, when combined with (3.26) and (3.27) and corrected for recombination effects, yields the following dimensionless relationship between T_a and T_e (6):

$$(3.29) \quad T_a = T_e + \frac{1.53 \times 10^4 \, (1+3/2T_e) T_e^3 \left[\frac{T_x}{T_e} + 2\right] \exp(-T_x/T_e) \left[(1-\alpha) - \rho\alpha 2 T_e^{-3/2} \exp(1/T_e)\right]}{\ln\left(\frac{DT_e^3}{\rho\alpha}\right)}$$

where:

$$(3.30) \quad D = \frac{9\chi^3 m_a}{4\pi e^6 \rho_c} = 0.2980$$

Since

$$\frac{\rho}{T_e^{3/2} \exp(-1/T_e)} \cong \frac{(1 - \alpha_*)}{\alpha_*^2}$$

near equilibrium where $T_e \tilde{=} T_a$, the term in square brackets may be rearranged to

$$\frac{(1 - \alpha)\ \alpha_*^2 - \alpha^2 (1 - \alpha_*)}{\alpha_*^2} \tag{3.31}$$

The following three flow situations are then possible:

a.) If $\alpha_* > \alpha$ then $T_a > T_e$ and ionization predominates.

b.) If $\alpha_* < \alpha$ then $T_a < T_e$ and recombination predominates.

c.) If $\alpha_* = \alpha$ then $T_a = T_e$ and the flow is in equilibrium.

IV NONDIMENSIONALIZING PARAMETERS

It is convenient to express the various governing equations in a dimensionless form. This is accomplished by referring all variables to constants which are characteristic to the particular problem. Such parameters for an ionizing gas are listed in the following table:

QUANTITY		FORMULA	UNITS	VALUE FOR ARGON
Temperature	T_c	χ/k	$^oK.$	183,000
Density	ρc	$\beta\, m_a(\chi/k)^{3/2}$	gm/cm^3	150
Pressure	p_c	$\beta(\chi/k)^{5/2}$	atmos.	5.65×10^7
Enthalpy	h_c	(χ/m_a)	erg/gm	3.78×10^{11}
Velocity	u_c	$\sqrt{\chi/m_a}$	cm/sec	6.17×10^5
Time	τ_c	$\left(\frac{m_a N_o}{\rho_c}\right)^2 \frac{1}{k_{rd}}$	sec	7.45×10^{-18}
Length	L_c	$u_c \times \tau_c$	cm	4.11×10^{-12}

The governing quasi-linear differential equations, rewritten in terms of dimensionless quantities (denoted by primes), become:

OVERALL CONTINUITY

$$\frac{\partial}{\partial s'}(\rho' u') + \rho' u' \frac{\partial \theta}{\partial n'} = 0 \tag{4.1}$$

S-MOMENTUM

$$u' \frac{\partial u'}{\partial s'} + \frac{1}{\rho'} \frac{\partial p'}{\partial s'} = 0 \tag{4.2}$$

N-MOMENTUM

$$u'^2 \frac{\partial \theta}{\partial s'} + \frac{1}{\rho'} \frac{\partial p'}{\partial n'} = 0 \tag{4.3}$$

EQUATION OF STATE

$$p' = \rho' (T_a' + \alpha T_e') \tag{4.4}$$

ENERGY

$$h' = 5/2 (T_a' + \alpha T_e') + \alpha \tag{4.5a}$$

$$H_o = h' + 1/2\, u'^2 = \text{Constant} \tag{4.5b}$$

SPECIES CONSERVATION

$$u' \frac{\partial \alpha}{\partial s'} = k_r' \rho'^2 \alpha \left[\frac{(1 - \alpha_*)}{\alpha_*^2} (1 - \alpha) - \alpha^2 \right] \tag{4.6}$$

RELATION BETWEEN T_e AND T_a

$$T_a' = T_e' + \frac{1.53 \times 10^4 (1+3/2T_e) T_e^3 \left[\frac{T_x}{T_e} + 2 \right] \exp(-T_x/T_e) \left[(1 - \alpha) - \rho\alpha^2 T_e^{-3/2} \exp(1/T_e) \right]}{\ln\left(\frac{DT_e^3}{\rho\alpha}\right)} \tag{4.7}$$

SAHA EQUATION

$$\frac{\alpha_*^2}{(1 - \alpha_*)} = \frac{T_x^{3/2}}{p'} \exp(-1/T_e') \tag{4.8}$$

SPEED OF SOUND

$$a'^2 = 5/3 (T_a' + \alpha T_e') \tag{4.9}$$

(4.10) $$k_r' = \left[\frac{T_x}{T_e'} + 2\right] \exp\left(\frac{T_{ion} - T_x}{T_e'}\right)$$

The first seven of these equations are to be solved simultaneously (in conjunction with the last three) for the seven unknowns.

$$p', \quad \rho', \quad T_a', \quad T_e', \quad \alpha, \quad u', \quad \theta$$

V SOLUTION BY THE METHOD OF CHARACTERISTICS

The simultaneous solution of the seven governing partial differential equations is accomplished by use of the Method of Characteristics. For steady flow, neglecting the effects of viscosity and heat transfer, the equations of motion admit a solution with an arbitrarily chosen set of normal derivatives on certain "characteristic" lines. Along characteristics, then, the governing equations are linearily dependent. While the normal derivatives along characteristics may be chosen arbitrarily, a compatibility relation relating the properties, exists along these lines. As a consequence, the properties may not be chosen independently. In gas dynamics these characteristic lines are called Mach lines, lines along which discontinuities in pressure and density propagate.

In nonequilibrium gas flows, the Mach lines are not the only lines along which the equations of motion admit arbitrary assignment of normal derivatives. Streamlines in such flows are also characteristic lines. While the governing equations determine the variation of entropy and velocity along a streamline, they do not determine the rate of change of these properties normal to the flow. Thus, discontinuities in velocity and entropy derivatives may exist normal to the streamlines. The gradients of entropy and velocity,

however, are not arbitrary if the entropy and total enthalpy are known along each streamline in the undisturbed flow.

The equations of the characteristic lines may be obtained by direct elimination among the equations of motion (18) or by matrix methods (17). Chu (9) has shown that the frozen speed of sound defines the slopes of the characteristic lines in reacting gas flows, and that these characteristic directions are:

(5.1) $$\frac{\partial n'}{\partial s'} = 0 \qquad \text{(streamline)}$$

(5.2) $$\frac{\partial n'}{\partial s'} = \pm \frac{1}{\sqrt{M^2 - 1}} \qquad \text{(Mach line)}$$

where M is the frozen Mach number. Analogous to perfect gas flow, a frozen Mach angle may be defined by:

(5.3) $$\tan \mu = \pm \frac{1}{\sqrt{M^2 - 1}}$$

Physically, μ is the angle between the velocity vector at a point and the Mach lines passing through the same point (Figure 2). By use of (5.3), the directional derivatives along the characteristic curves may be written as:

(5.4) (a) $$\frac{\partial}{\partial s'} = \frac{\partial}{\partial s'}$$

(b) $$\frac{\partial}{\partial \xi} = \frac{\sqrt{M^2 - 1}}{M} \frac{\partial}{\partial s'} + \frac{1}{M} \frac{\partial}{\partial n'}$$

$$(c)\quad \frac{\partial}{\partial \eta} = \frac{\sqrt{M^2 - 1}}{M} \frac{\partial}{\partial s'} - \frac{1}{M} \frac{\partial}{\partial n'}$$

The advantage of this method of solution is that all equations may be expressed as ordinary differential equations along the characteristic curves. The system of curvilinear coordinates to which the equations refer, however, is dependent upon the flow field itself.

Data along a single characteristic line does not specify enough information to uniquely define or determine the flow. Data must also be known along some other line which intersects a characteristic. In nonequilibrium Prandtl-Meyer flow, the state of the motion along the first Mach line is specified as being that of the undisturbed stream. Then, to complete the solution, properties along some other line which intersects this wave head must be known. The next section provides this data along the wall streamline at the corner.

VI SOLUTION FOR FROZEN FLOW

The time required for a fluid particle to traverse the sharp corner is infinitesimally small when compared to the chemical reaction time, so the flow in this region may be assumed to be frozen. The deviation of the temperature of the electron from that of the atom will be small if the initial state is in equilibrium. The flow in the immediate neighborhood of the corner is, then, frozen (hence it is isentropic) with equal electron and atom temperatures.

To obtain the solution for frozen flow, the governing equations must be written in characteristic form. The n-momentum equation and overall continuity equations will be transformed by use of the differentiation formulas derived in the last section.

The n-momentum equation (4.3) easily rearranged into the form:

$$(6.1) \qquad \frac{\sqrt{M^2 - 1}}{\rho' u'^2}\left[\frac{\partial p'}{\partial \xi} - \frac{\partial p'}{\partial \eta}\right] + \left[\frac{\partial \theta}{\partial \xi} + \frac{\partial \theta}{\partial \eta}\right] = 0$$

Rearrangement of (4.1) is accomplished by substitution from (4.2) for $\frac{\partial u'}{\partial s'}$ and replacing $\frac{\partial \rho'}{\partial s'}$ with the expression obtained by differentiating (4.4) partially with respect to s'. Eliminating $\frac{dT_d}{ds'}$ by use of the energy equation (4.5) and employing equation (5.4) yields the overall continuity equation in characteristic form:

$$(6.2) \qquad \frac{\sqrt{M^2 - 1}}{\rho' u'^2}\left[\frac{\partial p'}{\partial \xi} + \frac{\partial p'}{\partial \eta}\right] + \left[\frac{\partial \theta}{\partial \xi} - \frac{\partial \theta}{\partial \eta}\right] = -F$$

First adding and then subtracting (6.1) from (6.2) results in two ordinary differential equations relating p' and θ :

$$(6.3a) \qquad \frac{\sqrt{M^2 - 1}}{\rho' u'^2}\frac{dp'}{d\xi} + \frac{d\theta}{d\xi} = -F$$

$$(6.3b) \qquad \frac{\sqrt{M^2 - 1}}{\rho' u'^2}\frac{dp'}{d\eta} - \frac{d\theta}{d\eta} = -F$$

where: $$F = \frac{2\dot{w}'}{5 u' M (1 + \alpha) T'}$$

The frozen expansion of an ionized gas has no characteristic length contained either explicitly or implicitly within the problem. This absence of a characteristic length implies a complete independence of scale. Thus, the properties of the gas may be assumed to be constant along radial lines emanating from the sharp corner; i.e. $\frac{\partial}{\partial \eta} = 0$. The mass production rate, $\dot{w}'$, is identically zero since the composition is unchanging; hence for a frozen expansion:

$$(6.4) \qquad \frac{\sqrt{M^2 - 1}}{\rho' u'^2}\frac{dp'}{d\xi} + \frac{d\theta}{d\xi} = 0$$

Since it can be shown that a frozen flow is isentropic with a constant isentropic index γ :

$$(a) \qquad \frac{T_o}{T} = \left(1 + \frac{\gamma - 1}{2} M^2\right)$$

$$(6.2) \qquad (b) \qquad \frac{\rho_o}{\rho} = \left(1 + \frac{\gamma - 1}{2} M^2\right)^{1/\gamma - 1}$$

$$(c) \qquad \frac{p_o}{p} = \left(1 + \frac{\gamma - 1}{2} M^2\right)^{\gamma / \gamma - 1}$$

where the subscripts $_o$ represent stagnation values and $\gamma = 5/3$ for an ionized gas.

Substitution of (6.5c) and the equation of state into (6.4) gives:

$$(6.6) \qquad \mp d\theta = \frac{\sqrt{M^2 - 1}}{2 M^2} \frac{dM^2}{\left(1 + \frac{\gamma - 1}{2} M^2\right)}$$

Integration yields the solution for frozen corner flow with $T_e = T_a$ (26):

$$(6.7) \qquad \mp \theta = \tan^{-1}\left(\sqrt{M^2 - 1}\right) - \sqrt{\frac{\gamma + 1}{\gamma - 1}} \tan^{-1}\left[\sqrt{\frac{\gamma - 1}{\gamma + 1}\,(M^2 - 1)}\right]$$

Property variations along the wall streamline (at the corner) and along the wave head are now known. The solution for the nonequilibrium region is propagated from the intersection of these two curves.

In the nonequilibrium flow region $T_e \neq T_a$, so equations (6.3a) and (6.3b) will not apply there. By substitutions similar to those just discussed, it can be shown that the right side of (6.3a) and (6.3b) for nonequilibrium flow has the form:

$$(6.8) \qquad F = \frac{4 \dot{w}'}{5 u' M (T_a' + \alpha T_e')}$$

However, the Mach number in such case is based upon the speed of sound as given in (4.9) and thus depends upon $T_e \neq T_a$.

VII NUMERICAL INTEGRATION

In Section V it was shown that 3 characteristic lines pass through each point in the flow and that along these lines the governing equations become ordinary differential equations. The integration procedure begins with a knowledge of data at points (J, I) and (J+1, I-1) --refer to Figure 2. The location of point (J+1, I) is found by approximating the η and ξ characteristics through points (J, I) and (J+1, I-1), respectively, by their tangents, and calculating their intersection. The equations (6.3a) and (6.3b) may be integrated, simultaneously (by finite differences) along these tangent approximations of the η and ξ characteristics to yield the values of p and θ at their intersection, point (J+1, I). Knowing the value of θ allows the streamline to be approximated by its tangent. The intersection of this streamline with the "initial data line" (point s) is then calculated. Interpolation between the points at which data are known, (J, I) and (J+1, I-1), gives the values of the properties at point (s). The remaining equations may now be integrated along the streamline to obtain the first approximations of the values of the remaining properties at point (J+1, I).

The solution of the governing characteristic equations begins at the wave head; all properties along it being equal to their free stream (equilibrium) values. Since along this first Mach line, the

flow has experienced no deflection, i.e. $\theta = 0^o$, the angles $\delta_{1,I}$ are given by:

$$\delta_{1,I} = -\mu_1 = -\tan^{-1}\left[\frac{1}{\sqrt{M_1^2 - 1}}\right] \tag{7.1}$$

while in general these angles are determined from:

$$\delta_{J,I} = -\mu_{J,I} + \theta_{J,I} \tag{7.2a}$$

$$\delta_{J+1,I-1} = \mu_{J+1,I-1} + \theta_{J+1,I-1} \tag{7.2b}$$

The $_1$ subscript represents free stream or initial, i.e., M_1 is the free stream Mach number, etc.

The mesh size for this solution is determined by the distance ($\Delta r'$) between points on the wave head, and by the frozen Mach number increment ΔM in the frozen flow solution at the corner. For a given $\Delta r'$, the x-y coordinates of a general point on the wave head are:

$$x_{1,I} = I\,\Delta r' \cos\mu_1 \tag{7.3a}$$

$$y_{1,I} = I\,\Delta r' \sin\mu_1 \tag{7.3b}$$

With this information, the solution may be propagated into the nonequilibrium region.*

---

*At this point all quantities have been nondimensionalized, so all primes (') will be discontinued to simplify the writing of formulas.

In this step-by-step procedure, the characteristic lines at a point are approximated by their tangents given by (5.3). The coordinates of their point of intersection are given by (IIA-5) and (IIA-6) of Appendix II.

$$(7.4)\quad x_{J+1,I} = \frac{x_{J,I}\tan\delta_{J,I} - x_{J+1,I-1}\tan\delta_{J+1,I-1} + y_{J+1,I-1} - y_{J,I}}{\tan\delta_{J,I} - \tan\delta_{J+1,I-1}}$$

$$(7.5)\quad y_{J+1,I} = (y_{J+1,I-1}\tan\delta_{J,I} - y_{J,I}\tan\delta_{J+1,I-1} + (x_{J,I} - x_{J+1,I-1})\tan\delta_{J,I}\tan\delta_{J+1,I-1})/(\tan\delta_{J,I} - \tan\delta_{J+1,I-1})$$

Equations (6.3a) and (6.3b) are written in finite difference form and then solved simultaneously for p and θ. Thus:

$$(7.6)\quad p_{J+1,I} = \frac{C_{J,I}p_{J,I} + C_{J+1,I-1}p_{J+1,I-1} + \theta_{J+1,I-1} - \theta_{J,I} - F_{J,I} - F_{J+1,I-1}}{C_{J,I} + C_{J+1,I-1}}$$

$$(7.7)\quad \theta_{J+1,I} = (C_{J,I}C_{J+1,I-1}(p_{J+1,I-1} - p_{J,I}) + C_{J+1,I-1}\theta_{J,I} + C_{J,I}\theta_{J+1,I-1} + C_{J+1,I-1}F_{J,I} - C_{J,I}F_{J+1,I-1})/(C_{J,I} + C_{J+1,I-1})$$

where F is given by (6.8) and C represents $\sqrt{M^2 - 1}/\rho' u'^2$. The distances between points on the characteristic lines are:

$$(7.8)\quad \Delta\xi = \sqrt{(x_{J+1,I} - x_{J+1,I-1})^2 + (y_{J+1,I} - y_{J+1,I-1})^2}$$

$$(7.9)\quad \Delta\eta = \sqrt{(x_{J+1,I} - x_{J,I})^2 + (y_{J+1,I} - y_{J,I})^2}$$

Equations (7.6) and (7.7) give initial "guesses" of the values of p and θ at the unknown point (J+1, I), since the data at the points (J, I) and (J+1, I-1) are known.

Then, with $\theta_{J+1,I}$, the streamline through the point (J+1,I) is approximated by its tangent. The intersection of the streamline with a line joining the two points (J, I) and (J+1, I-1) is defined by the coordinates:

$$x_s = (x_{J,I}y_{J+1,I-1} - x_{J+1,I-1}y_{J,I} + (x_{J,I} - x_{J+1,I-1})$$
$$(x_{J+1,I}\tan\theta_{J+1,I} - y_{J+1,I}))/(y_{J+1,I-1} - y_{J,I} + \tag{7.10}$$
$$(x_{J,I} - x_{J+1,I-1})\tan\theta_{J+1,I})$$

$$y_s = \frac{x_{J,I}y_{J+1,I-1} - x_{J+1,I-1}y_{J,I} + (y_{J,I} - y_{J+1,I-1})x_s}{(x_{J,I} - x_{J+1,I-1})} \tag{7.11}$$

The flow properties at this intersection are obtained by linear interpolation between the two known points using the general formula:

$$(prop)_s = (prop)_{J+1,I-1} + \left(\frac{\text{length}}{\text{ratio}}\right)(prop_{J,I} - prop_{J+1,I-1}) \tag{7.12}$$

where the $\left(\frac{\text{length}}{\text{ratio}}\right)$ is defined by:

$$\left(\frac{\text{length}}{\text{ratio}}\right) = \sqrt{\frac{(x_s - x_{J+1,I-1})^2 + (y_s - y_{J+1,I-1})^2}{(x_{J,I} - x_{J+1,I-1})^2 + (y_{J,I} - y_{J+1,I-1})^2}} \tag{7.13}$$

To obtain the degree of ionization at point (J+1, I), the mass production equation may now be integrated along a streamline. In finite difference form, (4.6) becomes:

$$\alpha_{J+1,I} = \alpha_s + \dot{w}_s \frac{\Delta s}{u_s} \tag{7.14}$$

$\Delta s'$ is the nondimensional distance along a streamline:

$$\Delta s = \sqrt{(x_{J+1,I} - x_s)^2 + (y_{J+1,I} - y_s)^2} \tag{7.15}$$

Integration of the s-momentum equation:

$$u_{J+1,I} = u_s - \frac{(p_{J+1,I} - p_s)}{\rho_s u_s} \tag{7.16}$$

yields the unknown velocity, $u_{J+1,I}$.

The high degree of coupling among the equations of Section IV requires that T_e, ρ, and α be chosen as independent variables. Knowing these three properties at any point in the flowfield, all other properties may be calculated.

Data which is known at the new point, (J+1, I), at this stage of the solution include:

(1) coordinates of the point

(2) pressure

(3) flow deflection angle

(4) degree of ionization

(5) velocity

However, determination of other properties cannot be accomplished until the temperature T_e and density are known.

For the determination of this temperature, it is convenient to define a new variable:

$$\varphi = T_a + \alpha T_e \tag{7.17}$$

Its value at point (J+1, I) may be obtained by expressing the constancy of stagnation enthalpy along streamlines (equation (4.5b)). Thus:

(7.18) $\phi_{J+1,I} + 0.4((2.5\ \phi_s + \alpha_s) + 0.5\ (u_s^2 - u_{J+1,I}^2))$

The density may now be evaluated by use of the equation of state (4.4),

(7.19) $$\rho_{J+1,I} = \frac{p_{J+1,I}}{\phi_{J+1,I}}$$

The individual temperatures have yet to be determined, however.

Chain rule differentiation of (4.7) with respect to s' gives

(7.20) $$\frac{dT_a}{ds} = \frac{\partial T_a}{\partial T_e}\frac{\partial T_e}{\partial s} + \frac{\partial T_a}{\partial \rho}\frac{\partial \rho}{\partial s} + \frac{\partial T_a}{\partial \alpha}\frac{\partial \alpha}{\partial s}$$

Using this expression to eliminate $\frac{dT_a}{ds}$ from the logarithmic differentiated equation of state gives a differential equation expressing the rate of change to T_e along a streamline:

(7.21) $$\frac{dT_e}{ds} = (F_1 + \alpha)^{-1}\left[\frac{1}{\rho}\frac{dp}{ds} - (F_2 + \frac{\phi}{\rho})\frac{d\rho}{ds} - (F_3 + T_e)\frac{d\alpha}{ds}\right]$$

where F_1, F_2, and F_3 are defined on the next page.

The finite difference form of (7.21) becomes:

(7.25) (See added page)

the subscript $_s$ denoting the coefficients of the derivatives are evaluated at the point (s) (coordinates given by (7.10) and (7.11). With T_e, ρ and α known at (J+1, I), T_a may be evaluated there by use of equation (4.7). All other properties may be obtained by use of the appropriate equations.

(7.22) $$F_1 = \frac{\partial T_a}{\partial T_e} = \frac{1.53 \times 10^4 (1 - \alpha) \exp(-T_x/T_e)}{\alpha L^3} \left\{ L T_x^2 (1 + 1.5T_e) + \right.$$

$$\left. T_e T_x (4L - 3) + T_e T_x (7.5L - 4.5) + 6T_e^2 (L - 1) + T_e^3 (12L - 9) \right\} +$$

$$\frac{1.53 \times 10^4 \quad \rho \alpha \exp((1 - T_x)/T_e)}{L^2} \left\{ T_x T_e^{-1/2} (L-3) + T_x T_e^{1/2} \right.$$

$$(6L - 4.5) - 6T_e^{1/2} + T_e^{-1/2} (1.5T_x \; L - 2L) + T_e^{1/2} (7.5L - 9) +$$

$$\left. L T_x T_e^{-3/2} (T_x - 1) \right\}$$

(7.23) $$F_2 = \frac{\partial T_a}{\partial \rho} = \frac{1.53 \times 10^4}{\alpha \; L^2} (1 + 1.5T_e) T_e^3 \left[\frac{T_x}{T_e} + 2 \right] \exp(-T_x/T_e)$$

$$\left\{ (1 - \alpha)/\rho - \alpha^2 \quad T_e^{-1.5} \quad \exp(1/T_e)(L + 1) \right\}$$

(7.24) $$F_3 = \frac{\partial T_a}{\partial \alpha} = \frac{1.53 \times 10^4}{(\alpha L)^2} (1 + 1.5T_e) T_e^3 \left[\frac{T_x}{T_e} + 2 \right] \exp(-T_x/T_e)$$

$$\left\{ (1 - \alpha) - L - \alpha^2 \rho T_e^{-1.5} \exp(1/T_e)(L - 1) \right\}$$

where: $$L = \ln(D T_e^3 / \rho \alpha)$$

(7.25) $$T_{e_{J+1,I}} - T_{e_s} + 1./(F_1 + \alpha)_s \left[(p_{J+1,I} - p_s)/\rho_s - \right.$$

$$\left. (\phi/\rho + F_2)(\rho_{J+1,I} - \rho_s) - (T_e + F_3)_s (\alpha_{J+1,I} - \alpha_s) \right]$$

A first approximation to all the properties at point (J+1, I) is thus obtained. In the limit as the characteristic mesh becomes infinitesimally small, the solution approaches an "exact" solution. Any finite size mesh induces an error into the solution. One method normally used to reduce this inherent error is to replace the coefficients in the finite difference equations with average values, calculated from values of the properties at the points (J, I) and (J+1, I-1):

$$\text{coeff}^{(1)} = \left[\text{coeff}(\text{prop}_{J,I}^{(0)}) + \text{coeff}(\text{prop}_{J,I}^{(\text{calc})})\right]/2 \tag{7.26}$$

All calculations are then repeated. Presumably, if the mesh size is chosen small enough, this iterative technique would not appreciably increase the accuracy of the solution. In the calculations carried out for this thesis no iterations were employed, principally to conserve computation time.

VIII DISCUSSION

From Figure 6, it is seen that both T_e and T_a increase toward their equilibrium free stream values. The rate of increase of the electron temperature with respect to the radial coordinate is greater than the corresponding rate of increase of the atom temperature. That is:

$$\frac{dT_e'}{dr'} > \frac{dT_a'}{dr'}$$

so that for all r', $T_e' > T_a'$ as required for a recombining flow. This behavior was discussed in Section III-7. Typical deviations of T_a from T_e along various η characteristics (the wave head dor-responds to $\eta = 1$) are given below:

	r' ($\times 10^{11}$)	θ_w (^{o})	T_e' ($\times 10$)	T_a' ($\times 10$)	$(T_e - T_a)$ (^{o}K.)	% of T_e'
15	2.54	-3.17	.66036	.65219	150	1.24
25	1.35	-5.34	.62944	.61351	293	2.54
50	2.17	-10.39	.59700	.56500	405	3.75
75	2.34	-14.90	.54980	.52370	477	4.75

θ_w is the flow deflection angle at the wall for the η characteristic. For flow deflection angles less than -5^o, T_e may be assumed equal T_a. The difference between T_e and T_a increases to 5% for a wall angle of 15^o. For larger flow deflection angles, this deviation would probably be much greater.

Comparing the data with those of Reference (16) is quite interesting. Along any η characteristic, the two temperature gas ($T_e \neq T_a$), as considered in this thesis, reaches its equilibrium state in half the radial distance required for nonequilibrium flow with $T_e = T_a$ as considered in (16). The wave tail ($\eta = 75$) as calculated in (16) is plotted in Figure 6 for comparison. At $r' = 2.5 \times 10^{11}$ (4.6 cm.), the difference in T_a for the two methods is 620°K. or 5.45%. The values of pressure and degree of ionization are also underestimated by the $T_e = T_a$ nonequilibrium approach.

Reference to Figure 10 shows that for the initial conditions cited $T_e \cong T_a$ throughout the expansion fan. Since M, T', and α were all increased, it is not known which of these input variables was responsible for this near equilibrium phenomena. Comparison with results of (6), however, shows that as the stagnation temperature is increased, T_e more closely approximates T_a. It will be noticed that for this case, equilibrium is approached at an even faster rate the data of Case I. The dependence of the flow on these initial parameters will be discussed later.

Figure 7 demonstrates the dependence of pressure upon the radial distance from the corner. As the temperature, the pressure increased toward its free stream value. The pressure gradient radially along any η characteristic is greater than those from Glass' work, thus equilibrium is reached closer to the corner. The

model of reference (16) underestimated the pressure at a radial distance of $r' = 2.5 \times 10^{11}$ (4.6 cm.) by $.14 \times 10^{-7}$, or nearly 0.79 atmospheres. This is a difference of 20% compared to the free stream pressure of 3.65 atmospheres.

That the departure from equilibrium is less than that predicted by Glass and Takano is demonstrated in Figure 8. If $T_e \neq T_a$ in the analysis, the minimum degree of ionization is 0.0829 while the cited reference gives a value of 0.0748. This large difference may be explained by reference to Figure 6 and equation (3.23). The temperature predicted by reference (16) is below that of this analysis. From equation (3.23):

$$k_r' = \left[\frac{T_x}{T_e} + 2\right] \exp\left(\frac{T_{ion} - T_x}{T_e}\right)$$

then, $k_r' (T_e = T_a) > k_r' (T_e \neq T_a)$. This higher rate of recombination allows the flow to reduce its degree of ionization below that of this work. For the sake of comparison, at $r' = 2.5 \times 10^{11}$, $k_{r=}'$ = 990 while $k_{r\neq}' = 709$.

The ionization of Case I decreased by 9.1% of the total at the point of minimum ionization, while in Case II it decreased by only 4%. The calculations showed that the rate of recombination for Case I is two to three times that of Case II. For all r', the temperature calculated in Case II is greater than the corresponding temperature calculated in Case I. Equation (3.23) then predicts $k_{r\,II}' > k_{r\,I}'$.

Case		θ_w	r' ($\times 10^{-11}$)	$k_{r'}$ ($\times 10^{-3}$)
I	5	- 0.922	.308	.631
II	5	- 0.844	.308	.278
I	30	- 6.40	.137	1.000
II	35	- 6.73	.140	.397
I	60	-12.25	1.589	.734
II	70	-12.66	1.577	.288

The atom and electron temperatures at a constant radial distance from the corner are plotted as a function of the local deflection angle in Figures 9 and 13. The value of r' chosen (6.3×10^{10}) is near the point at which the effects of nonequilibrium are a maximum for Case I. However, this value of the radial coordinate is near the equilibrium region for all η in Case II. A value of $r' = 2.4 \times 10^{10}$ yields larger temperature differences in this case.

Case	r' ($\times 10^{-10}$)	θ (^{o})	$(T_e - T_a)$ (^{o}K.)
I	6.3	-9.5	275
II	6.3	-7.8	128
II	2.4	-11.5	280

To achieve the same difference of atom and electron temperatures, the gas in Case II had to expand 2^o further than in Case I.

All the data reported herein were calculated on an IBM 7040 computer in the FORTRAN IV programming language. The size of the characteristic mesh determines the accuracy of the results. Values of $\Delta r' = 6 \times 10^9$ and $\Delta M = 0.01$ were used in this work,

while reference (16) used $\Delta r' = 2 \times 10^9$ and $\Delta M = 0.01$. For a wall angle of -15^o, 45 minutes of computation time was required to complete the description of the flowfield.

The differences between the results presented in this thesis and those reported in reference (16) were largely produced by the different mathematical models chosen to represent ionized argon. Other factors influencing the results are the different size characteristic mesh and the different integration scheme. The use of an iterative technique should improve the accuracy of the results reported here. A third reason for differences arises from the changes in formulation required by considering a two temperature gas. As an example, the value of F in (6.3a) and (6.3b) was changed from $\frac{2\dot{w}'}{5u'M(1+\alpha)T'}$ to $\frac{4\dot{w}'}{5u'M(T_a + \alpha T_e')}$. It was the latter form which was used to integrate (7.6) and (7.7) along the characteristic curves. Reference (16) employed the former value of F for this task. Also, the expression for the speed of sound assumed a different form:

$$a_{(T_a \neq T_e)} = \sqrt{5/3(T_a' + \alpha T_e')} \qquad a_{(T_a = T_e)} = \sqrt{5/3\,(1+\alpha)T'}$$

The directions of the characteristic curves, being dependent solely on the Mach number, could have been greatly affected.

Some correspondence of data may be made with that of Bray and Wilson (6). The initial data for their computations compares well

well with that reported in this thesis.

Case I	$p = 3.66$ atm	$T = 12{,}500^{o}K.$	$\alpha = 0.09$
Bray	$p_o = .57$	$T_o = 11{,}000$	$\alpha = 0.066$
Case II	$p = 1.65$ atm	$T = 15{,}000^{o}K.$	$\alpha = 0.50$
Bray	$p_o = .57$	$T_o = 16{,}500$	$\alpha = 0.90$

Comparing the results of Case II with Figure 5 in (6) shows that the same difference in $(T_e - T_a)$ will be obtained by expanding argon through a conical nozzle with an area ratio of 3. This corresponds approximately to $\theta_w = -15^{o}$ considered here.

Reference (6) also shows that reducing the stagnation temperature increases the separation of T_e and T_a. Figures 6 and 10 show this same result. The behavior of the degree of ionization as presented in reference (6) also closely approximates that shown in Figure 12.

During the writing of this thesis, Teare (24) reported a factor of 2 error in the work of Petschek and Byron (23) which increased the numerical constant in (3.18) to 8.8×10^{-6}. This error was not corrected in Bray and Wilson's analysis of the dependence of the atom temperature upon that of the electron. A detailed investigation of the effect of this error upon the results presented in this thesis has not been completed. However, the inclusion of this factor decreases the characteristic time (τ_c) and length (L_c) as well as the numerical constant of equation (3.29) to half the value reported here. Increased

by a factor of two are the constants of equations (3.18) through (3.22). The effect of this error is to increase the difference between T_e and T_a and to increase the radial derivatives of both temperatures.

IX CONCLUSION

It has been demonstrated that the temperatures of the atoms and electrons do not differ significantly from one another in the nonequilibrium flow of argon around a sharp corner. However, assuming that they are equal gives a solution which underestimates the temperature, pressure, and degree of ionization as shown in Figures 6 through 9. It seems essential, then, that in future investigations that the assumption of equal atom and electron should not be made.

The results presented in this thesis also suggest other problems which should be investigated:

(1) The solution should be carried out using smaller step sizes for the numerical integration, together with an iterative technique, such as described on page 29. A disadvantage of such an investigation is the lengthening of an already long computation time.

(2) The effects of the factor of 2 error reported by Teare (24) should be investigated.

(3) A determination of the effect of varying the initial parameters (M, T*, α) upon the flow field should be made.

(4) The calculations should be carried for larger wall angles. The increased expansion of the flow will increase the difference between the electron and atom temperatures significantly.

DATA

Property	Value Case I	Case II
M	1.76	2.0
T_a' T_e'	0.068369	0.0820
α	0.09123	0.500
ρ'	8.675×10^{-7}	2.373×10^{-7}
p'	6.472×10^{-8}	2.920×10^{-8}
h'	2.777×10^{-1}	8.075×10^{-1}
u'	6.206×10^{-1}	9.055×10^{-1}
a'	3.5262×10^{-1}	4.528×10^{-1}
k_r'	6.076×10^{2}	2.74×10^{2}

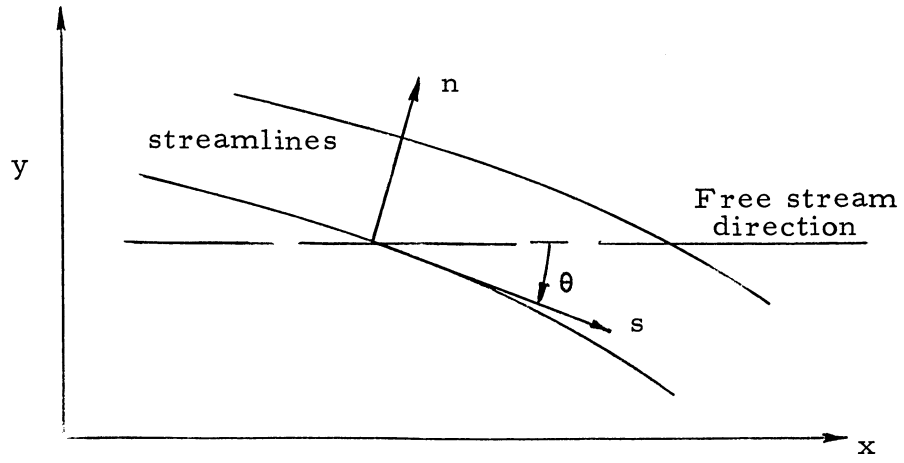

NORMAL STREAMLINE COORDINATE SYSTEM
(Figure 1)

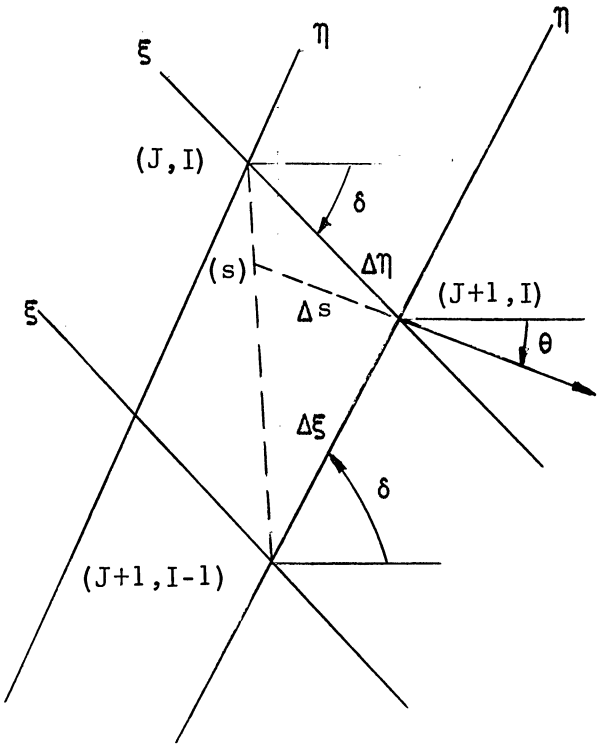

CHARACTERISTIC MESH
(Figure 2)

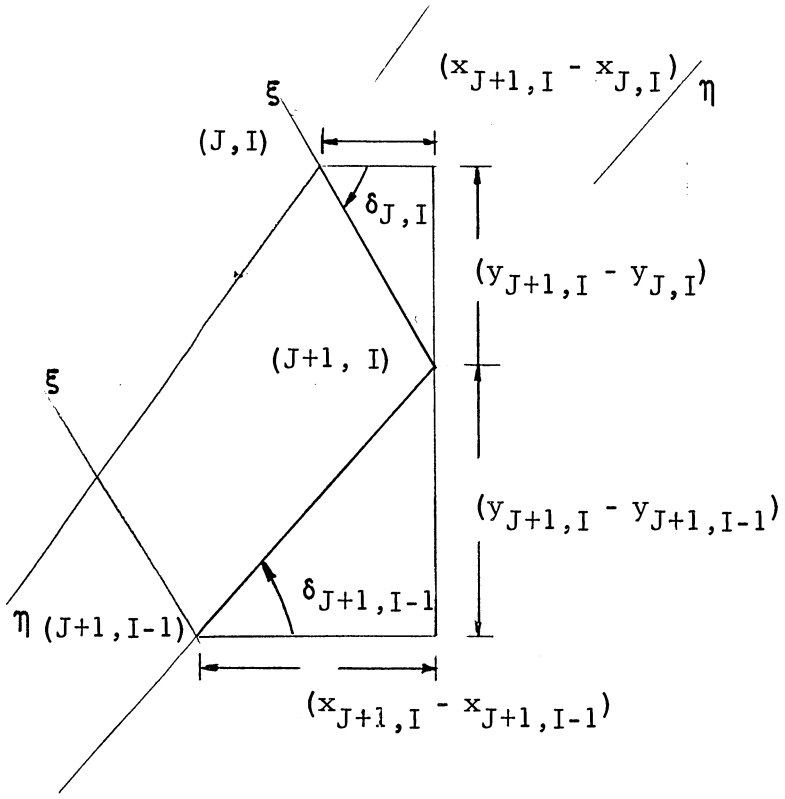

COORDINATES OF POINT (J+1,I)
(Figure 3)

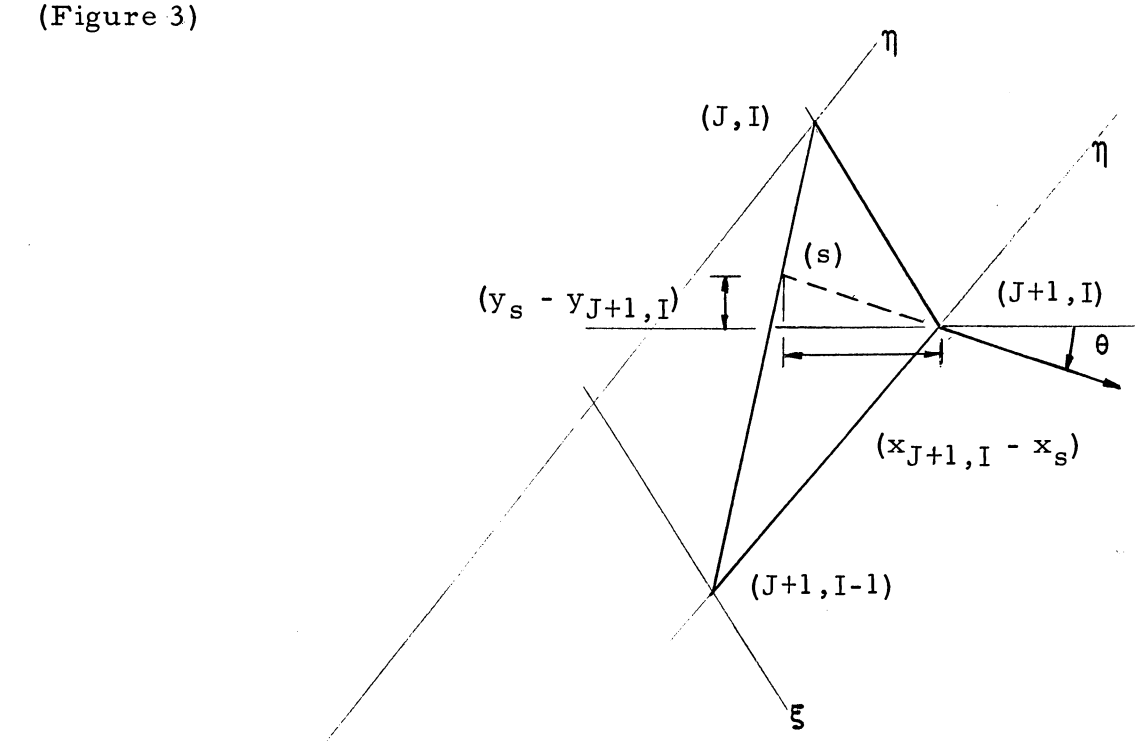

COORDINATES OF THE STREAMLINE INTERSECTION (s)
(Figure 4)

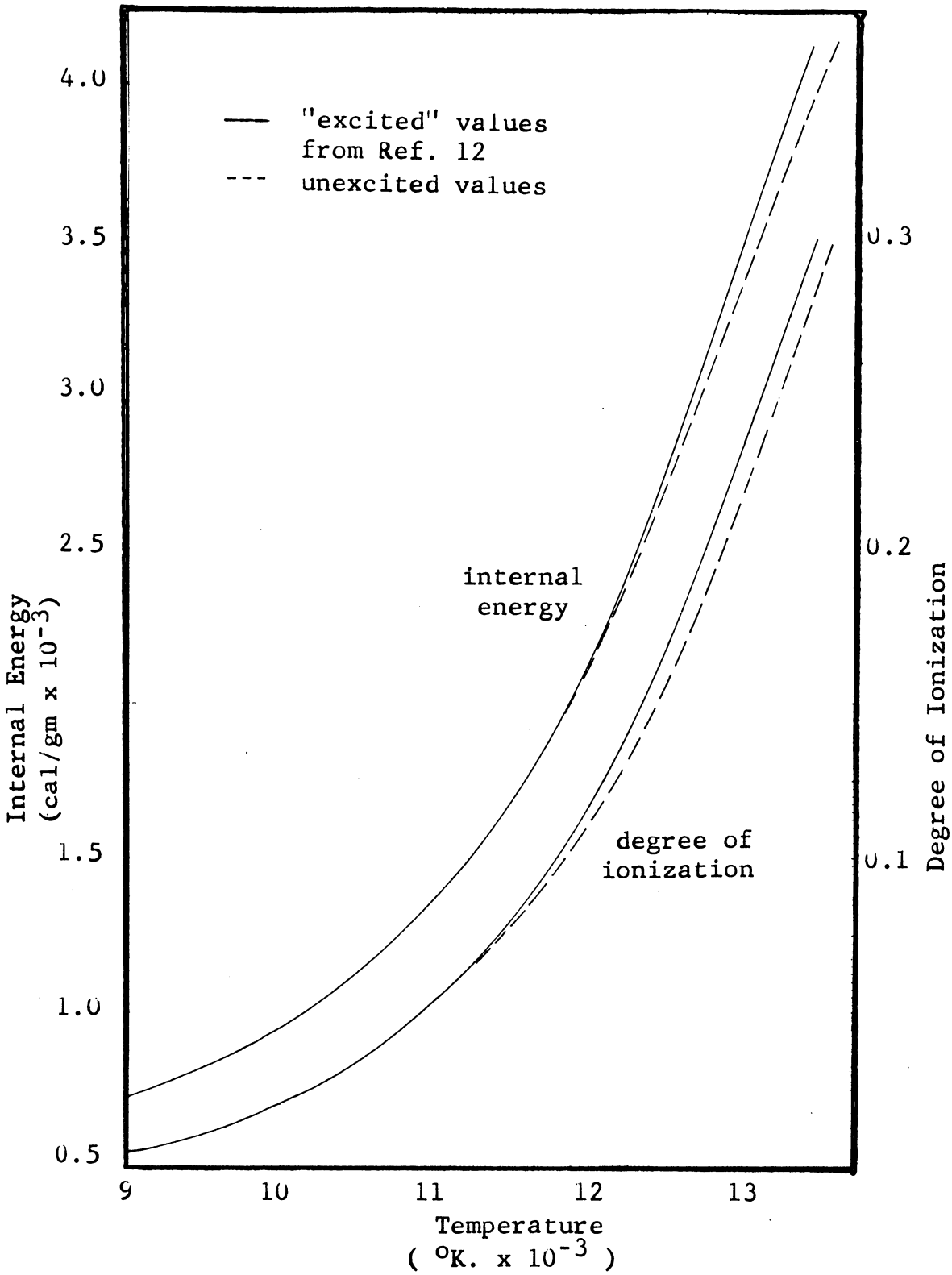

Internal Energy and Equilibrium Composition versus Temperature

Figure 5

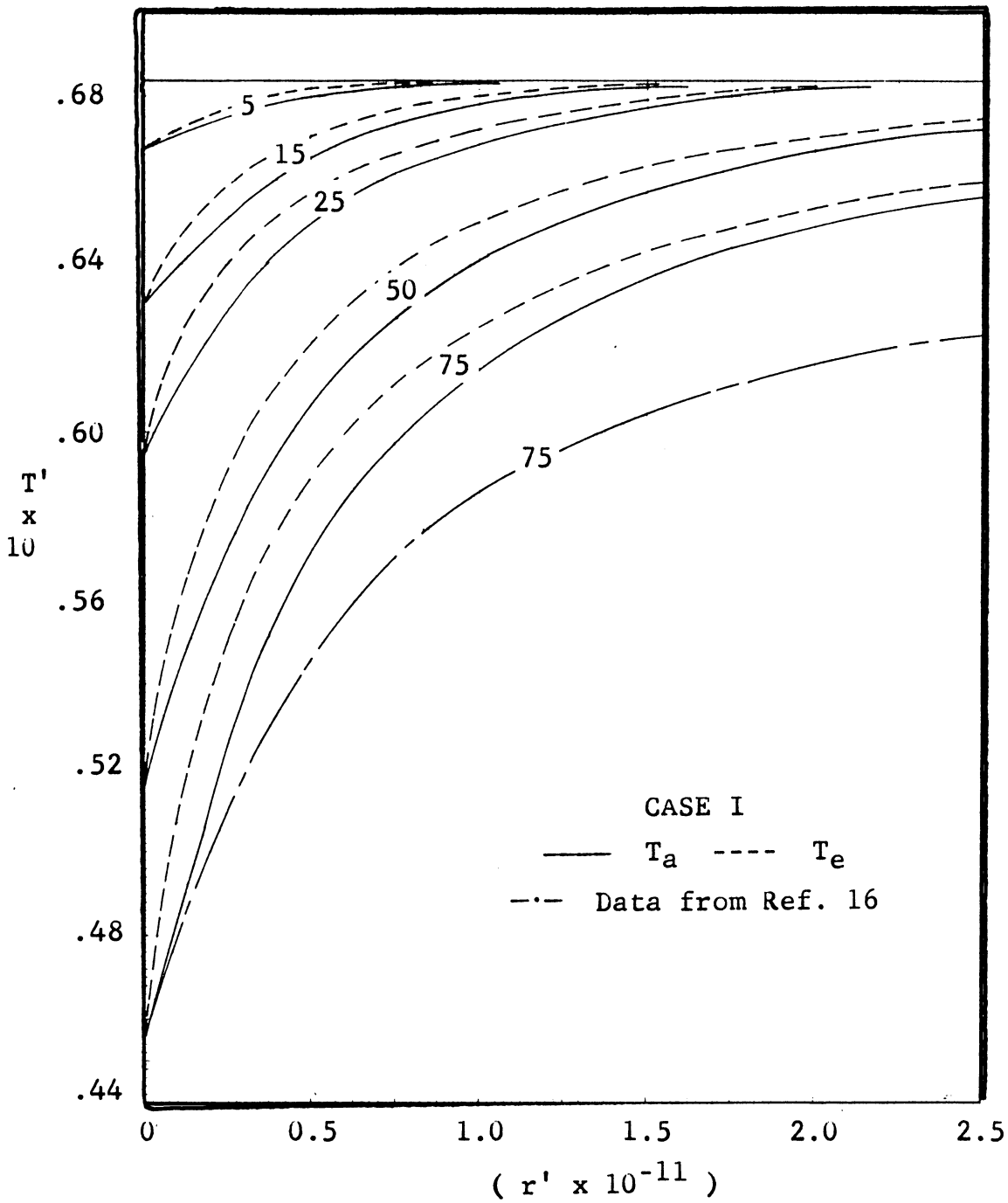

Temperature versus radial coordinate

Figure 6

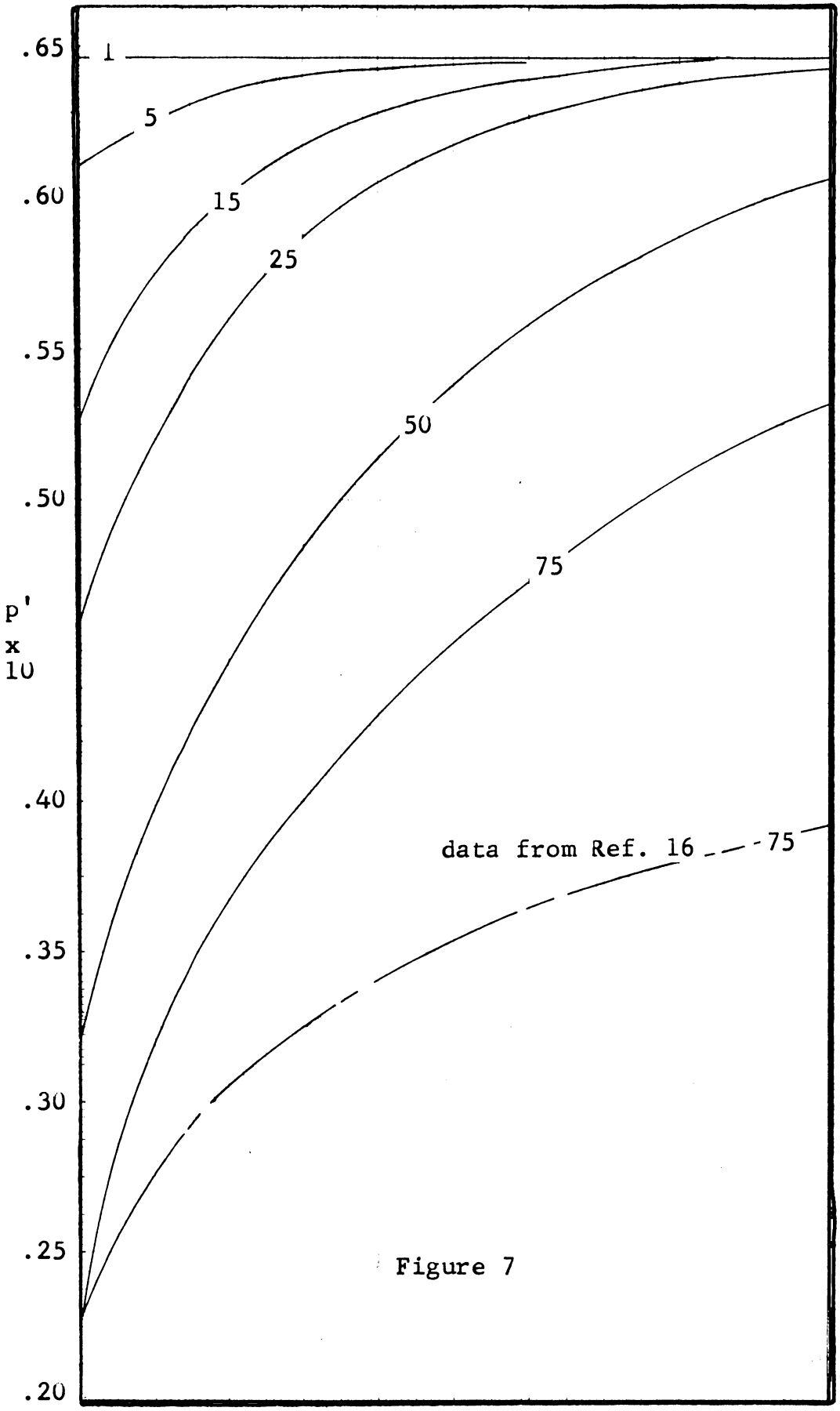

Figure 7

Pressure versus radial coordinate

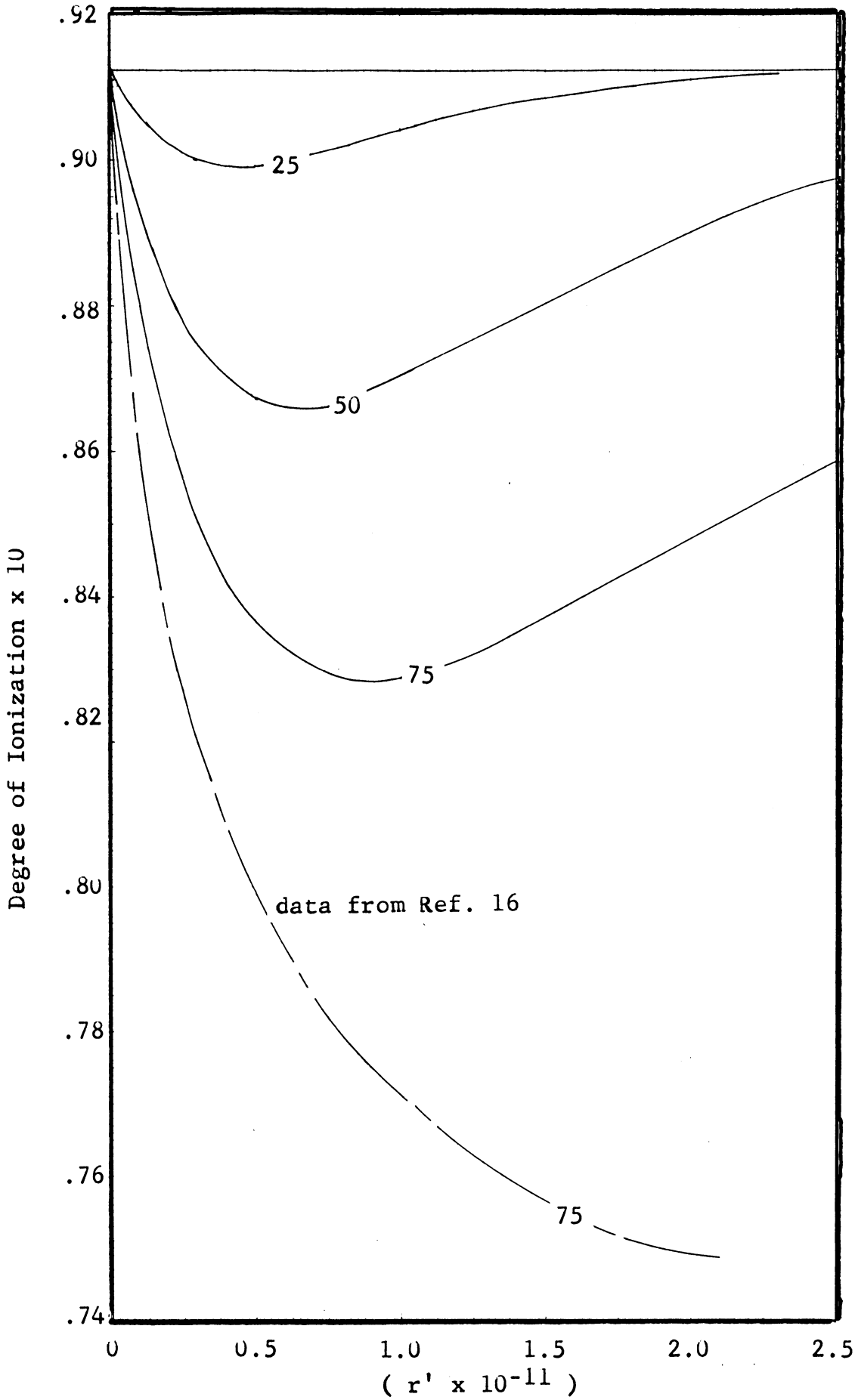

Degree of Ionization versus radial coordinate

Figure 8

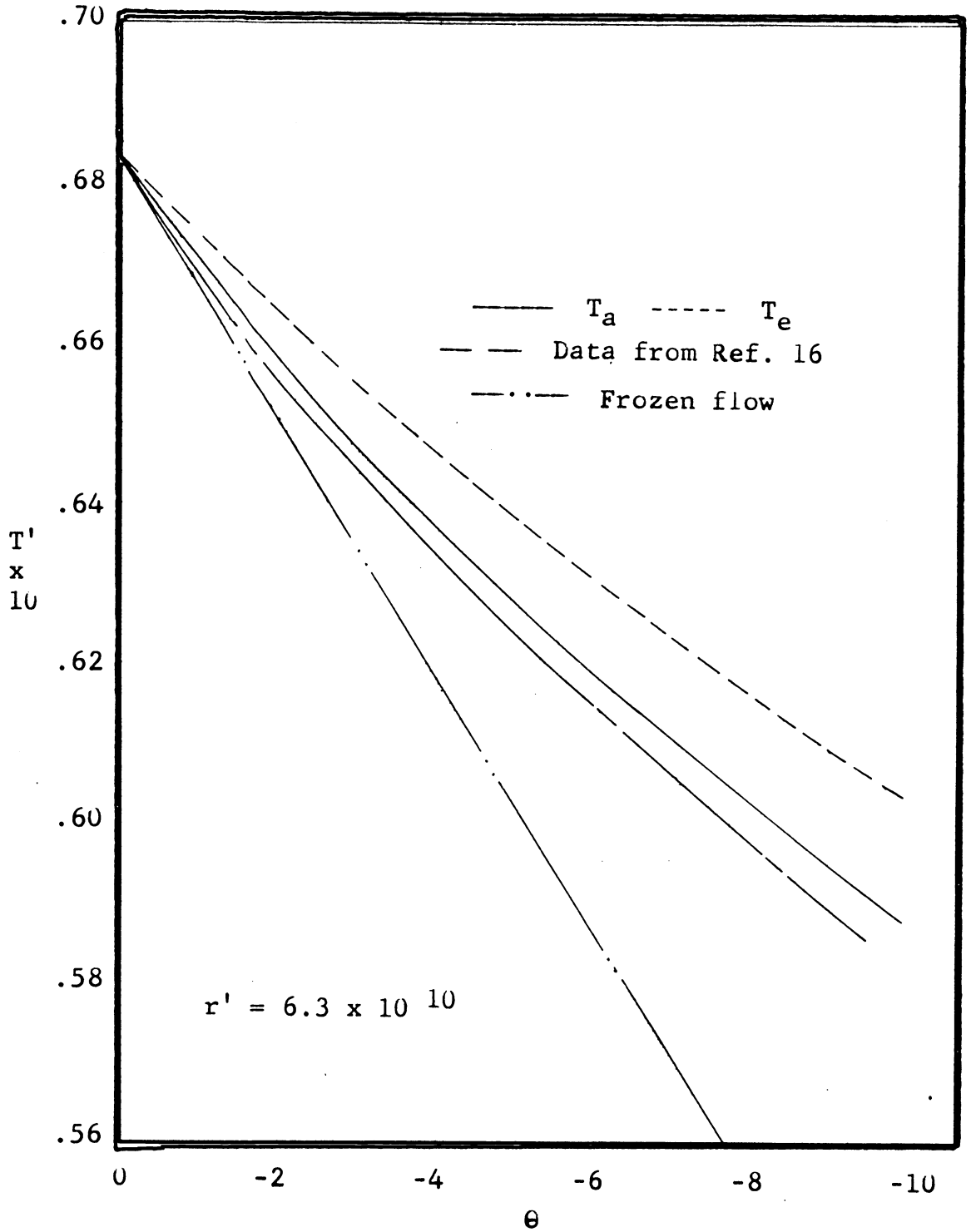

Temperature at a constant radial distance versus local flow deflection angle

Figure 9

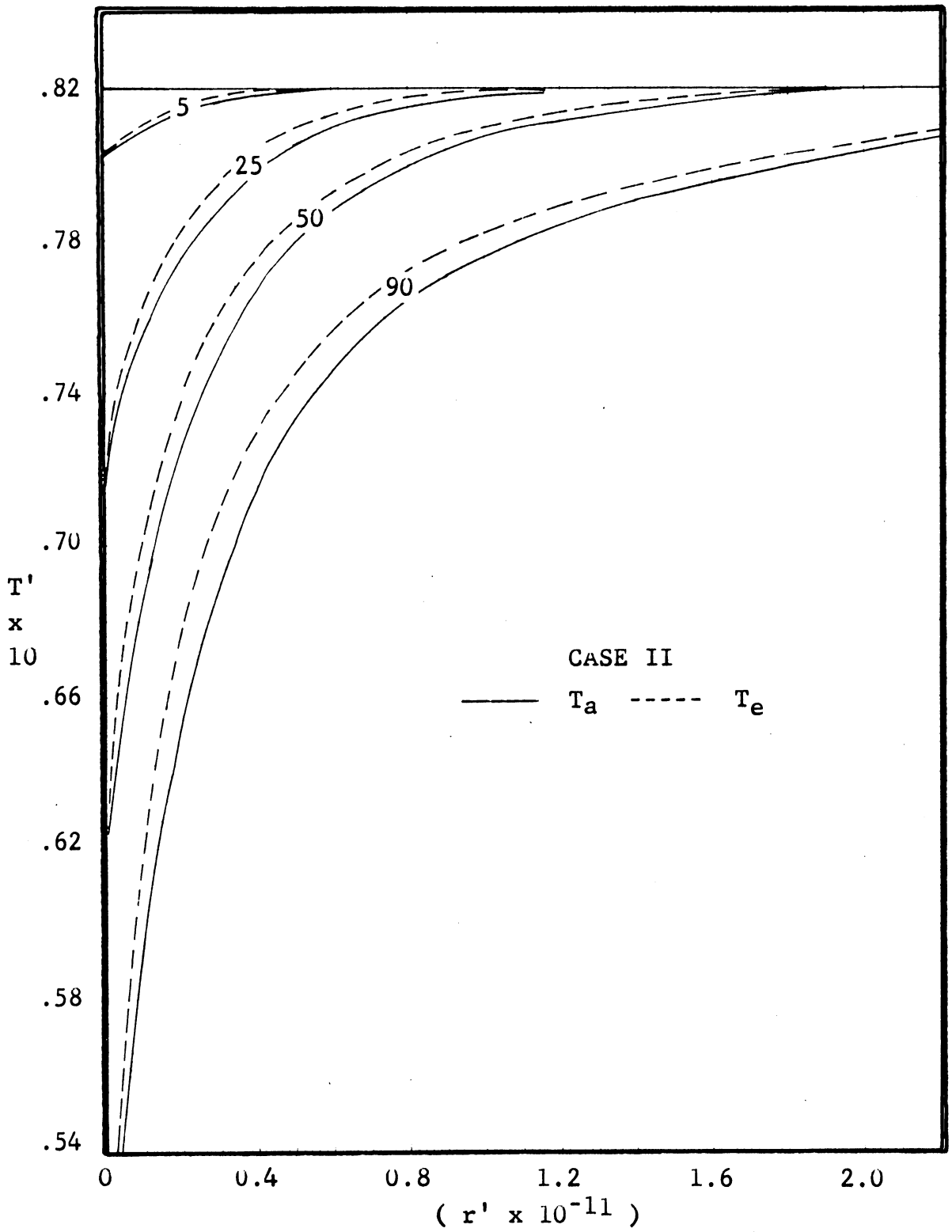

Temperature versus radial coordinate

Figure 10

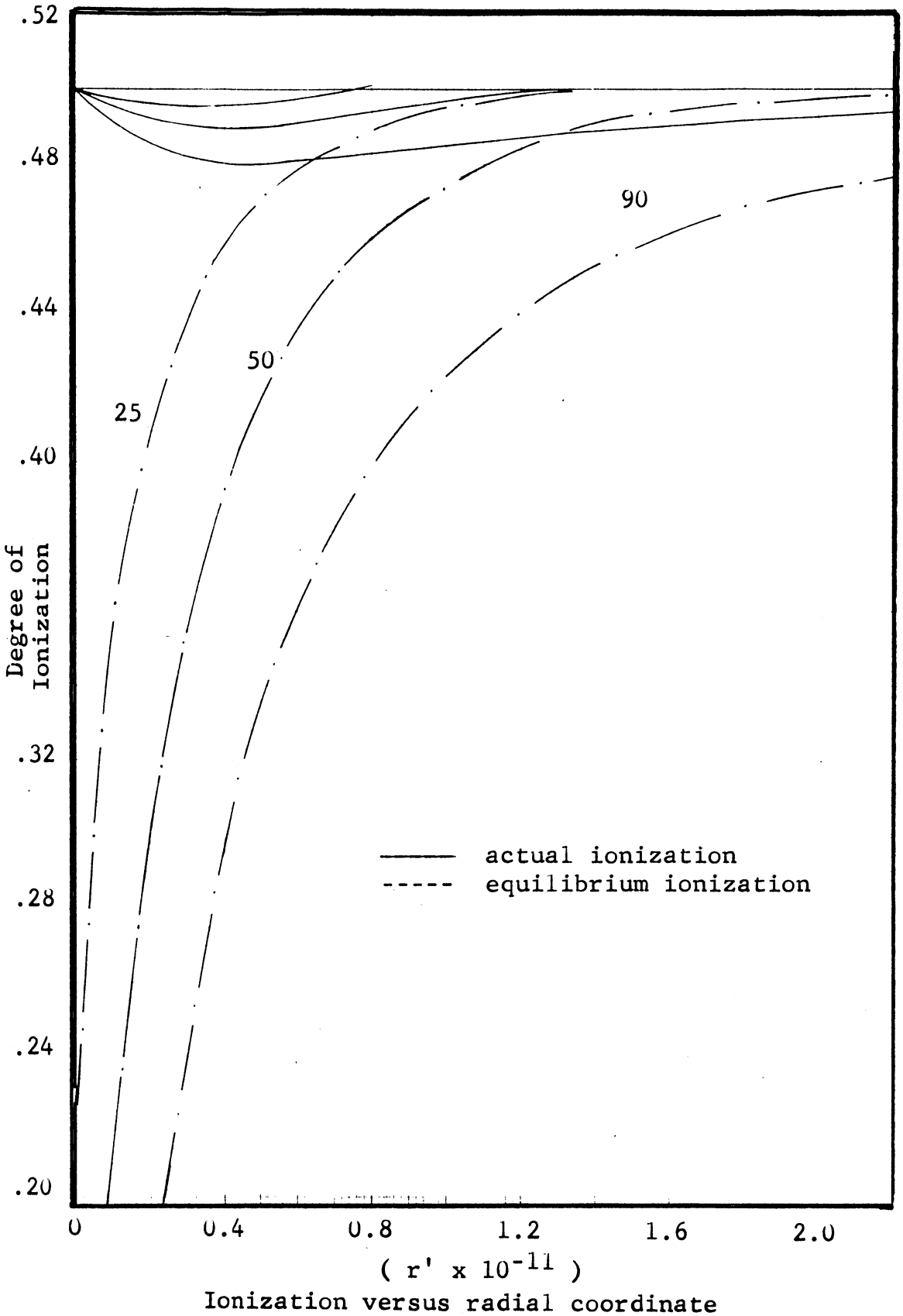

Ionization versus radial coordinate

Figure 11

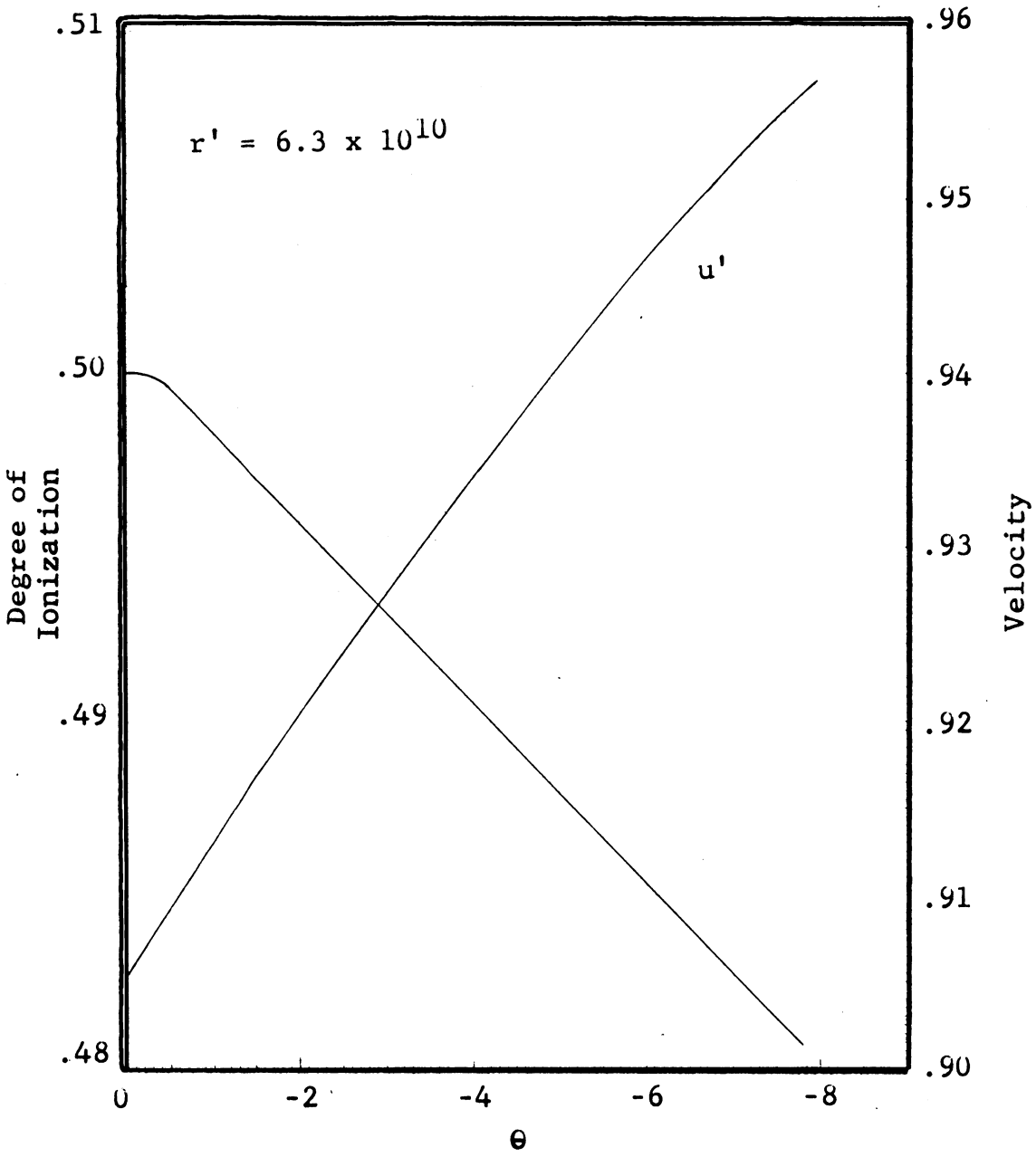

Degree of Ionization and Velocity
at a constant radial distance
versus local flow deflection angle

Figure 12

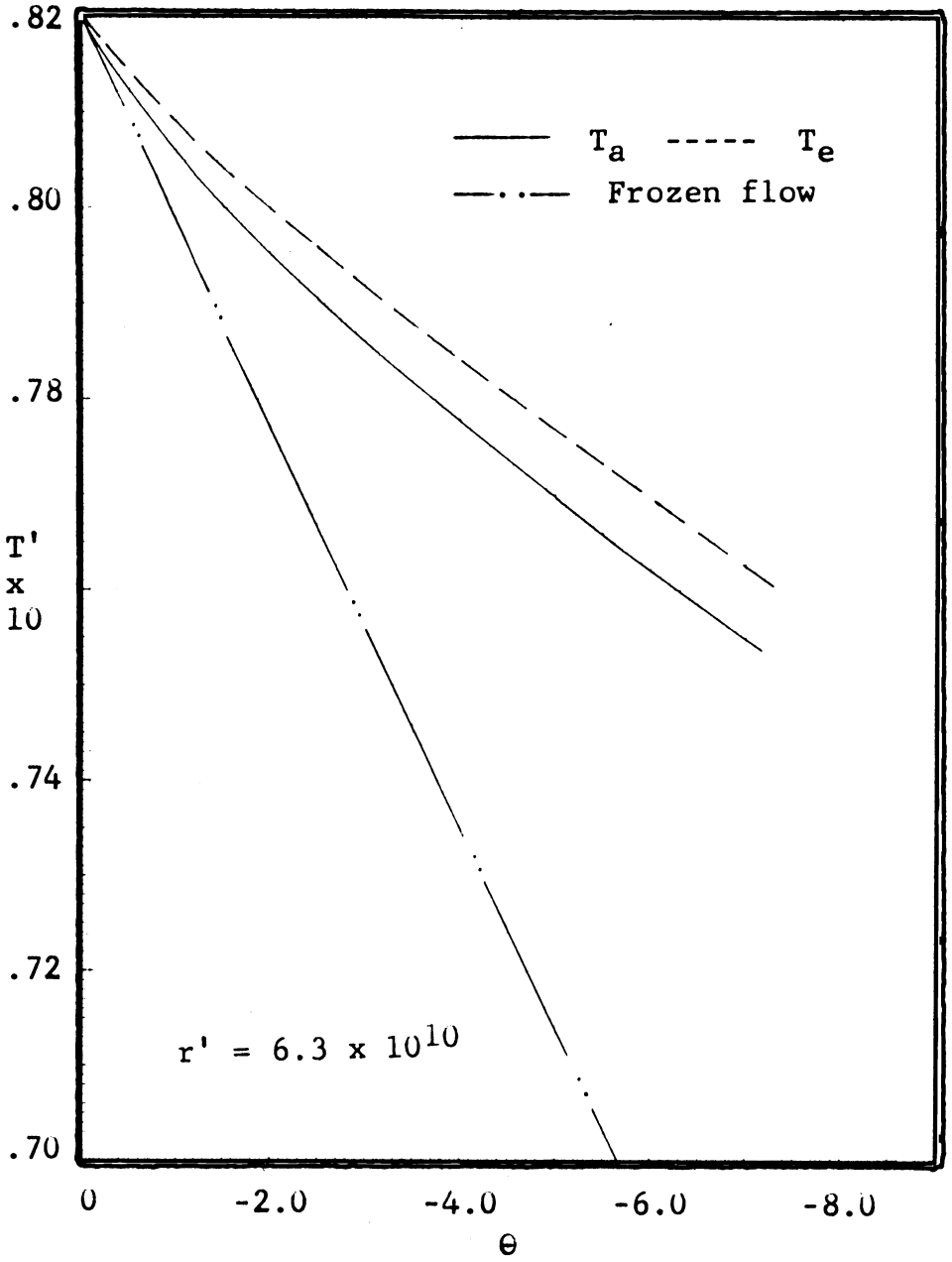

Temperature at a constant radial distance versus local flow deflection angle

Figure 13

REFERENCES

1. Biondi, M.A., "Afterglow Atomic Collision Processes, AD415829, August 20, 1963.

2. Biondi, M.A., "Electron-Ion and Ion-Ion Recombination", AD418411, September 19, 1963.

3. Bond, J.W., "Structure of a Shock Front in Argon", Phys. Rev., 105, 1957.

4. Bray, K.N.C., "Electron-Ion Recombination in Argon Flowing Through a Supersonic Nozzle", AASU Report No. 213, March, 1962.

5. Bray, K.N.C., and Wilson, J.A., "A Preliminary Study of Ionic Recombination of Argon in Wind Tunnel Nozzles", C.P.N. No. 559, Feb., 1960.

6. Bray, K.N.C., and Wilson, J.A., "A Preliminary Study of Ionic Recombination of Argon in Wind Tunnel Nozzles Part II", C.P.N. No. 634, 1963.

7. Calcote, H.F., "Relaxation processes in Plasma", Phys. Rev., 107, 1957.

8. Cambel, A.B., "Plasma Physics and Magnetofluidmechanics", McGraw-Hill Book Co., New York, 1963.

9. Chu, Boa-Teh, "Wave Propagation and the Method of Characteristics in Reacting Gas Mixtures with Application to Hypersonic Flow", WADC TN 57-213, Division of Engineering, Brown University, 1957.

10. Cleaver, J.W., "The Two Dimensional Flow of an Ideal Dissociation Gas", The College of Aeronautics Cranfield Report No. 123, Dec., 1959.

11. Dougal, A.A. and Goldstein, L., "Energy Exchange Between Electron and Ion Gases Through Coulomb Collisions in Plasmas", Phys. Rev., 109, Feb. 1, 1958.

12. Drellishak, K.S., Knopp, C.F., and Cambel, A.B., "Partition Functions and Thermodynamic Properties of Argon Plasma", AEDC-TDR-63-146, Aug., 1963.

13. Ford, L.R., "Differential Equations", McGraw-Hill Book Co., Inc., New York, 1955.

14. Galipeau, J., and Takano, A., "A Digital Computer Program for Calculating Nonequilibrium Expansion Flows of Dissociated Oxygen and Ionized Argon Around a Corner", UTIAS Tech. Note #69, August, 1963.

15. Glass, I.I., and Takano, A., "Nonequilibrium Expansion of Dissociated Oxygen Around a Corner", UTIA Rept. #91, June, 1963.

16. Glass, I.I., and Takano, A., "Nonequilibrium Expansion Flow of Ionized Argon Around a Corner", UTIAS Rept. #95, Sept., 1963.

17. Glass, I.I., and Dawada, H., "Prandtl-Meyer Flow of Dissociated and Ionized Gases", UTIA Rept. #85, June, 1962.

18. Howarth, L. (Editor), "Modern Developments in Fluid Dynamics-High Speed Flow", Oxford at the Clarendon Press, Oxford, 1953.

19. Laport, O., "High Temperature Shock Waves", Combustion and Propulsion, Third A.G.A.R.G. Colloquium, Pergamon Press.

20. Leob, L.B., "Kinetic Theory of Gases", McGraw-Hill Book Co., Inc, New York, 1927.

21. Li, T.Y., "Recent Advances in Nonequilibrium Dissociating Gas Dynamics", Ad 252392, Dec., 1960.

22. McCracken, D.D., "A Guide to Fortran Programming", John Wiley and Sons, Inc., New York, 1961.

23. Petschek, H., and Hyron, S., "Approach to Equilibrium Ionization Behind Strong Shock Waves in Argon", Annals of Physics, Vol.

24. Schuler, K. (Editor), "Ionization in High Temperature Gases", Progress in Astronautics and Aeronautics Vol. 12, Academic Press, New York, 1963.

25. Sears, W.R. (Editor), "General Theory of High Speed Aerodynamics", Princeton University Press, Princeton, N.J., 1954.

26. Shapiro, A.H., "The Dynamics and Thermodynamics of Compressible Fluid Flow Vol I", The Ronald Press Co., New York, 1953.

27. Wierum, F.A., Jr., "Prandtl-Meyer Expansion of an Ionizing Monatomic Gas", Ph.D. Thesis, Rice University, May, 1962.

APPENDIX I ENERGY OF THE EXCITED STATE

The energy of a gaseous system is most easily obtained from the use of partition functions. While the energy of any particle of species is equal to the sum of the energies of its various degrees of freedom:

$$E_i = E_i^{tr} + E_i^{rot} + E_i^{vib} + E_i^{elec} \tag{I.1}$$

the total partition function is represented by:

$$Z_i = Z_i^{tr} \quad Z_i^{rot} \quad Z_i^{vib} \quad Z_i^{elec} \tag{I.2}$$

The monatomic atom possesses no rotational or vibrational degrees of freedom, so $Z_i^{vib} = Z_i^{rot} = 1$, simplifying (I.2).

The translational partition function, Z_i^{tr}, is obtained from quantum mechanics by a simple integration over phase space. The result is:

$$Z_i^{tr} = V\left[\frac{2\pi m_i k T_i}{h^2}\right]^{3/2} \tag{I.3}$$

where V is the volume of the system and h is Planck's constant ($=6.624 \times 10^{-27}$ erg.sec)

From its definition, the electronic partition function may be written as:

$$(I.4) \quad Z_i^{elec} = g_i^o \exp(-\epsilon_i^o/kT_i) \sum_j g_i^j \exp(-(\epsilon_i^j - \epsilon_i^o)/kT_i)$$

where g_i^j is the degeneracy of species i in energy level j, and ϵ_i^j is the energy of the j^{th} state (obtained by solution of Schroedinger's equation or from spectroscopic measurements). Logically, ϵ_i^o is the excess energy of the i^{th} species over an arbitrarily chosen reference energy level, and g^o is the degeneracy of this energy state.

The assumption of neglecting excited states requires that:

$$(I.5) \quad Z_i^{elec} = g_i^o \exp(-\epsilon_i^o/kT_i)$$

from which the total partition function of the unexcited i^{th} species becomes:

$$(I.6) \quad Z_i = V g_i^o \left[\frac{2\pi m_i kT_i}{h^2}\right]^{3/2} \exp(\epsilon_i^o/kT_i)$$

If the infinite sum, equation (I.4), is expanded, it takes the form:

$$(I.7) \quad Z_i = g_i^o \exp(-\epsilon_i^o/kT_i) + g_i^1 \exp(-\epsilon_i^1/kT_i) + ... + ...$$

The classical problem of the divergence of this series may be surmounted by including only the first few energy levels. This procedure introduces an error which increases with increasing temperature;

but this error is always small if the neglected energy states are much greater than kT.

The inclusion of excited states requires knowledge of the energy levels and their degeneracy. For this specific example, argon, the electronic partition functions for the three species, each referred to its own ground state, may be approximated by:

$$Z_a^{elec} = 1 + 60 \exp(-162{,}500/T_a) \tag{I.8}$$

$$Z_{a+}^{elec} = 4 + 2 \exp(-2062/T_{a+}) + 2 \exp(-156{,}560/T_{a+}) \tag{I.9}$$

$$Z_e^{elec} = g_e^{o} = 2 \tag{I.10}$$

The ground state degeneracy of the electron is 2 because of its spin. The assumption of all particles being in their ground state gives:

$$\begin{aligned} g_a^{o} &= 1 \\ g_{a+}^{o} &\tilde{=} 6 \\ g_e^{o} &= 2 \end{aligned} \tag{I.11}$$

If the particle partition functions are formed by use of (I.2) and (I.3) with (I.8), (I.9), or (I.10) and these results differentiated by use of equation (2.1), the internal energy of one particle of each species is obtained. Taking the ground state of the atom as the reference energy level ($\epsilon_a^{o} = 0$) and summing over all particles gives the specific, excited, equilibrium internal energy as:

$$\bar{e} = 3/2\, RT_* \left[(1 - \alpha)\, E_1 + \alpha\, E_2 + \alpha \right] + \frac{\alpha \chi}{m_a} \qquad \text{cal/gm} \tag{I.12}$$

where

$$E_1 = \frac{1 + 60 \exp(-162{,}500/T_*) + 6.5 \times 10^6 \exp(-162{,}500/T_*)}{1 + 60 \exp(-162{,}500/T_*)} \tag{I.13}$$

and

$$E_2 = \frac{2 + (1 + 1361/T_*) \exp(-2060/T_*)}{2 + \exp(-2060/T_*) + \exp(-156{,}560/T_*)} \tag{I.14}$$

APPENDIX II

(A) COORDINATES OF THE POINT (J+1, I)

Solution of this problem by the Method of Characteristics requires that the coordinates of certain points, defined by the intersection of characteristic curves, be known. From this data, physical distances along these characteristics may be determined, thus allowing the equations of Section VII to be integrated. Approximating the characteristic lines by their tangents (see Figure 3) at the points (J, I) and (J+1, I-1), two algebraic equations are obtained. These two equations may be simultaneously solved for $x_{J+1,\,I}$, and $y_{J+1,\,I}$ as demonstrated below:

(IIA-1) $$\tan\ \delta_{J,I} = (y_{J+1,I} - y_{J,I})/(x_{J+1,I} - x_{J,I})$$

(IIA-2) $$\tan\ \delta_{J+1,I-1} = (y_{J+1,I} - y_{J+1,I-1})/(x_{J+1,I} - x_{J+1,I-1})$$

may be rearranged to:

(IIA-3) $$x_{J+1,I}\tan\ \delta_{J,I} - x_{J,I}\tan\ \delta_{J,I} = y_{J+1,I} - y_{J,I}$$

(IIA-4) $$y_{J+1,I} = (x_{J+1,I} - x_{J+1,I-1})\tan\delta_{\ J+1,I-1} + y_{J+1,I-1}$$

which yield upon solution:

(IIA-5) $$x_{J+1,I} = \frac{x_{J,I}\tan\delta_{\ J,I} - x_{J+1,I-1}\tan\ \delta_{J+1,I-1} + y_{J+1,I-1} - y_{J,I}}{\tan\delta_{\ J,I} - \tan\delta_{\ J+1,I-1}}$$

(IIA-6) $$y_{J+1,I} = (y_{J+1,I-1}\tan\ \delta_{J,I} - y_{J,I}\tan\ \delta_{J+1,I-1} + (x_{J,I} - x_{J+1,I-1})\tan\ \delta_{J,I}\tan\ \delta_{J+1,I-1})/(\tan\delta_{\ J,I} - \tan\ \delta_{J+1,I-1})$$

(B) THE STREAMLINE INTERSECTION (s)

Several of the equations of Section VII are integrated along the streamline characteristic, so data must be known at some point upstream from (J+1, I). This data is obtained from a linear interpolation between points (J, I) and (J+1, I-1) as demonstrated by equation (7.12). The coordinates of the intersection of the streamline with a line joining these two points must be known in order to evaluate (7.13) as well as to integrate (7.14) and (7.16). Evaluation of (7.7) yields the value of $\theta_{J+1,I}$, from which the streamline may be approximated by its tangent through the point (J+1, I). The coordinates desired are determined by the simultaneous solution of the following two equations:

$$\text{(IIB-1)} \qquad \frac{(y_s - y_{J+1,I-1})}{(x_s - x_{J+1,I-1})} = \frac{(y_{J,I} - y_{J+1,I-1})}{(x_{J,I} - x_{J+1,I-1})}$$

$$\text{(IIB-2)} \qquad (y_s - y_{J+1,I})/(x_s - x_{J+1,I}) = \tan\theta_{J+1,I}$$

which gives:

$$\text{(IIB-3)} \qquad x_s = (x_{J,I}y_{J+1,I-1} - x_{J+1,I-1}y_{J,I} + (x_{J,I} - x_{J+1,I-1})(x_{J+1,I}\tan\theta_{J+1,I} - y_{J+1,I})) / (y_{J+1,I-1} - y_{J,I} + (x_{J,I} - x_{J+1,I-1})\tan\theta_{J+1,I})$$

$$\text{(IIB-4)} \qquad y_s = \frac{x_{J,I}y_{J+1,I-1} - x_{J+1,I-1}y_{J,I} + (y_{J,I} - y_{J+1,I-1})x_s}{(x_{J,I} - x_{J+1,I-1})}$$